Contribution of competition for light to within-species variability in stomatal conductance

Michael M. Loranty,[1,2] D. Scott Mackay,[1] Brent E. Ewers,[3,4] Elizabeth Traver,[3,5] and Eric L. Kruger[6]

Received 16 April 2009; revised 23 December 2009; accepted 28 December 2009; published 18 May 2010.

[1] Sap flux (J_S) measurements were collected across two stands dominated by either trembling aspen or sugar maple in northern Wisconsin. Observed canopy transpiration ($E_{C\text{-}obs}$) values derived from J_S were used to parameterize the Terrestrial Regional Ecosystem Exchange Simulator ecosystem model. Modeled values of stomatal conductance (G_S) were used to determine reference stomatal conductance (G_{Sref}), a proxy for G_S that removes the effects of temporal responses to vapor pressure deficit (D) on spatial patterns of G_S. Values of G_{Sref} were compared to observations of soil moisture, several physiological variables, and a competition index (C_I) derived from a stand inventory, to determine the underlying cause of observed variability. Considerable variability in G_{Sref} between individual trees was found, with values ranging from 20 to 200 mmol m^{-2} s^{-1} and 20 to 100 mmol m^{-2} s^{-1} at the aspen and maple stands, respectively. Model-derived values of G_{Sref} and a sensitivity to D parameter (m) showed good agreement with a known empirical relationship for both stands. At both sites, G_{Sref} did not vary with topographic position, as indicated by surface soil moisture. No relationships were observed between G_{Sref} and tree height (H_T), and a weak correlation with sapwood area (A_S) was only significant for aspen. Significant nonlinear inverse relationships between G_{Sref} and C_I were observed at both stands. Simulations with uniform reductions in incident photosynthetically active radiation (Q_0) resulted in better agreement between observed and simulated E_C. Our results suggest a link between photosynthesis and plant hydraulics whereby individual trees subject to photosynthetic limitation as a result of competitive shading exhibit a dynamic stomatal response resulting in a more conservative strategy for managing hydrologic resources.

Citation: Loranty, M. M., D. S. Mackay, B. E. Ewers, E. Traver, and E. L. Kruger (2010), Contribution of competition for light to within-species variability in stomatal conductance, *Water Resour. Res.*, *46*, W05516, doi:10.1029/2009WR008125.

1. Introduction

[2] Stomata function to regulate plant hydraulics and concurrently control carbon dioxide exchange between the biosphere and atmosphere. Accurate estimates of stomatal conductance are essential to model water and carbon cycles from local to global scales [*Bonan*, 1991; *Denning et al.*, 2003; *Famiglietti and Wood*, 1994; *Foley et al.*, 1996; *Kuchment et al.*, 2006; *Landsberg and Waring*, 1997; *Running and Coughlan*, 1988]. Estimates of stomatal conductance for species or plant functional types are typically obtained at the leaf or whole plant level using gas exchange and sap flux measurements, respectively, and scaled as required for specific model applications. Homogeneity within species or functional groups is implicit in current scaling methods, which until recently have been relatively limited by data acquisition [*Mackay et al.*, 2002; *Williams et al.*, 2004; *Wullschleger et al.*, 2001]. A number of recent studies have demonstrated varying degrees of heterogeneity in forest transpiration at the stand or hillslope scale [*Adelman et al.*, 2008; *Kumagai*, 2008; *Loranty et al.*, 2008; *Traver et al.*, 2010; *Tromp-van Meerveld and McDonnell*, 2006]. Understanding the drivers and mechanistic underpinnings of spatial and temporal variation in stomatal control of transpiration is crucial to improve scaling and predictive understanding of water and carbon fluxes.

[3] Stomata close to prevent hydraulic failure at high atmospheric vapor pressure deficit (D) in response to increased leaf water potential that is caused by high transpiration rates [*Mott and Parkhurst*, 1991]. This response occurs because high transpiration rates as a result of high D are responsible for hydraulic stress that can be lethal if unrestricted [*Sperry et al.*, 1998; *Tyree and Sperry*, 1989]. When D and light are low, stomata exhibit a linear response

[1]Department of Geography, State University of New York at Buffalo, Buffalo, New York, USA.
[2]Now at Woods Hole Research Center, Falmouth, Massachusetts, USA.
[3]Department of Botany, University of Wyoming, Laramie, Wyoming, USA.
[4]Program in Ecology, University of Wyoming, Laramie, Wyoming, USA.
[5]Now at Department of Biological Sciences, Dartmouth College, Hanover, New Hampshire, USA.
[6]Department of Forest Ecology and Management, University of Wisconsin-Madison, Madison, Wisconsin, USA.

0043-1397/10/2009WR008125

to photosynthetic photon flux density (Q_0) to maximize carbon uptake for productivity. Stomatal conductance (G_S) has been described as a response to key environmental drivers [*Jarvis*, 1976] that can be expressed as a function of plant hydraulics [*Oren et al.*, 1999b], and alternatively as a function of photosynthetic carbon uptake [*Ball et al.*, 1987]. Subsequently several models varying in complexity have been developed that define stomatal conductance in terms plant hydraulics. The following model defines G_S using Darcy's law [*Whitehead and Jarvis*, 1981; *Whitehead et al.*, 1984]:

$$G_S = K_S \frac{A_S}{A_L} \frac{1}{D} (\psi_S - \psi_L - h\rho_\omega g) \quad (1)$$

where G_S is canopy average stomatal conductance (mmol m^{-2} s^{-1}), K_S is whole tree hydraulic conductance (mmol m^{-2} s^{-1} MPa^{-1}), A_S is sapwood area (m^2), A_L is leaf area (m^2), D is vapor pressure deficit, ψ_S is soil water potential (MPa), ψ_L is leaf water potential (MPa), $h\rho_w g$ is the gravitational pull (g) on the water column of height (h) and density (ρ_w). Recently G_S (mmol m^{-2} s^{-1}) has been described solely by its saturating response to D in terms of reference stomatal conductance (G_{Sref}) (mmol m^{-2} s^{-1}), which is G_S at D = 1 kPa [*Katul et al.*, 2009; *Oren et al.*, 1999b]:

$$G_S = G_{Sref} - m \ln D \quad (2)$$

where $m = -\partial G_S / \partial \ln D$ is interpreted as stomatal sensitivity to D. In mesic environments a proportional relationship between G_S and sensitivity to D, where $m = 0.6\ G_{Sref}$ has been observed within and between species [*Addington et al.*, 2004; *Ewers et al.*, 2001; *Oren et al.*, 1999a, 1999b; *Wullschleger et al.*, 2002]. Species that exhibit this relationship regulate transpiration in order to maintain critical minimum leaf water potential and prevent run away cavitation, and are referred to as isohydric [*Franks et al.*, 2007; *Tardieu and Simonneau*, 1998].

[4] Recent studies at a variety of sites [*Adelman et al.*, 2008], including the ones used in the present study [*Loranty et al.*, 2008; *Traver et al.*, 2010], have shown that spatial variability in transpiration changes temporally in response to D. Briefly, at low D under minimal hydraulic stress G_S and thus canopy transpiration (E_C) are relatively homogeneous. However, individual trees exhibit differing responses to increasing D, and so greater variability in E_C is observed during midday periods of high D. Thus, for isohydric plants it is ideal to use G_{Sref} as a proxy for direct comparison of stomatal function between individuals because the effects of D are removed. This allows the effects of other variables, such as soil moisture, edaphic factors, or incident radiation (i.e., equations (1) and (2)), on variability in G_S to be examined more explicitly, without the confounding effects of temporal changes in D on spatial patterns of G_S.

[5] Decreases in sap flow velocity per unit xylem area (J_S) as a result of declines in soil moisture, indicating a stomatal response to hydraulic stress, have been reported in the literature for a variety of species [*Gazal et al.*, 2006; *Lagergren and Lindroth*, 2002; *Oren and Pataki*, 2001; *Pataki et al.*, 2000]. Topography, soil composition, and soil depth can contribute to soil moisture heterogeneity and have been linked to spatial variation in E_C during transitions between wet and dry periods [*Granier et al.*, 2000; *Tromp-van Meerveld and McDonnell*, 2006]. However, recent work at the sites used for this study suggest that variability in soil properties or soil moisture do not contribute to variability in E_C [*Traver et al.*, 2010].

[6] Plant hydraulics and photosynthetic capacity have recently been linked empirically [*Brodribb and Feild*, 2000; *Maherali et al.*, 2008] and theoretically [*Katul et al.*, 2003] in studies that seek to explain different strategies of hydraulic regulation and elucidate further the mechanisms responsible for stomatal regulation. Fractions of absorbed incident and diffuse radiation vary according to branching patterns, leaf distribution, leaf angle and orientation, and crown morphology [*Campbell and Norman*, 1998; *Cescatti*, 1998; *Ewers et al.*, 2007b]. Developmental light environment has been shown to impact leaf photosynthetic capacity [*Niinemets et al.*, 2004], and so competitive shading between crowns can be considered as a source of variability photosynthetic capacity among individuals. Potential sources of variability in factors contributing to light limited of photosynthesis can thus be considered in the context of plant hydraulics and the implications for G_S. Particularly decreased light availability through shading, as this has been shown to affect G_S [*Ewers et al.*, 2007b]. Additionally, competitive shading may be explored as a mechanistic explanation for the connection between spatial and temporal patters of transpiration mentioned above [*Loranty et al.*, 2008; *Traver et al.*, 2010].

[7] The following study has been conducted to test three hypotheses: (1) Within species, G_{Sref} exhibits spatial variation across stands, (2) G_{Sref} remains isohydric within species despite spatial variability, and (3) competition for light contributes to variability in G_{Sref}. We accomplish this using sap flux data, leaf gas exchange, and a model with coupled hydraulic and photosynthetic constraints on G_S. The goal is to elucidate the mechanisms responsible for variable stomatal control of biosphere-atmosphere gas exchange.

2. Methods

2.1. Site Description

[8] The study was conducted at two forest stands near the town of Park Falls in northern Wisconsin (45.95°N, 90.27°W) (Figure 1). Both stands are located within the Chequamegon-Nicolet National Forest less than 2 km from the WLEF Ameriflux tower, and associated with the Chequamegon Ecosystem Atmosphere Study (ChEAS) [*Bakwin et al.*, 1998; *Davis et al.*, 2003]. Topography in the area is gently rolling and the dominant geomorphic features in the area are outwash, pitted outwash, and moraines. The climate of the region is characterized by a long winter and a short growing season with mean January and July temperatures of −12°C and 19°C, respectively [*Fassnacht and Gower*, 1997].

[9] The first site chosen for this study, hereafter referred to as aspen, captures a forested wetland-to-upland transition dominated by speckled alder (*Alnus incana* (DuRoi) Spreng) and white cedar (*Thuja occidentalis L.*) in the wetland, and quaking aspen (*Populus tremuloides* Michx) in the upland. The aspen stand was a regenerating clear-cut area approximately 20 years old. The aspen study site measures 120 m × 120 m with an elevation gradient of ~3 m across the site.

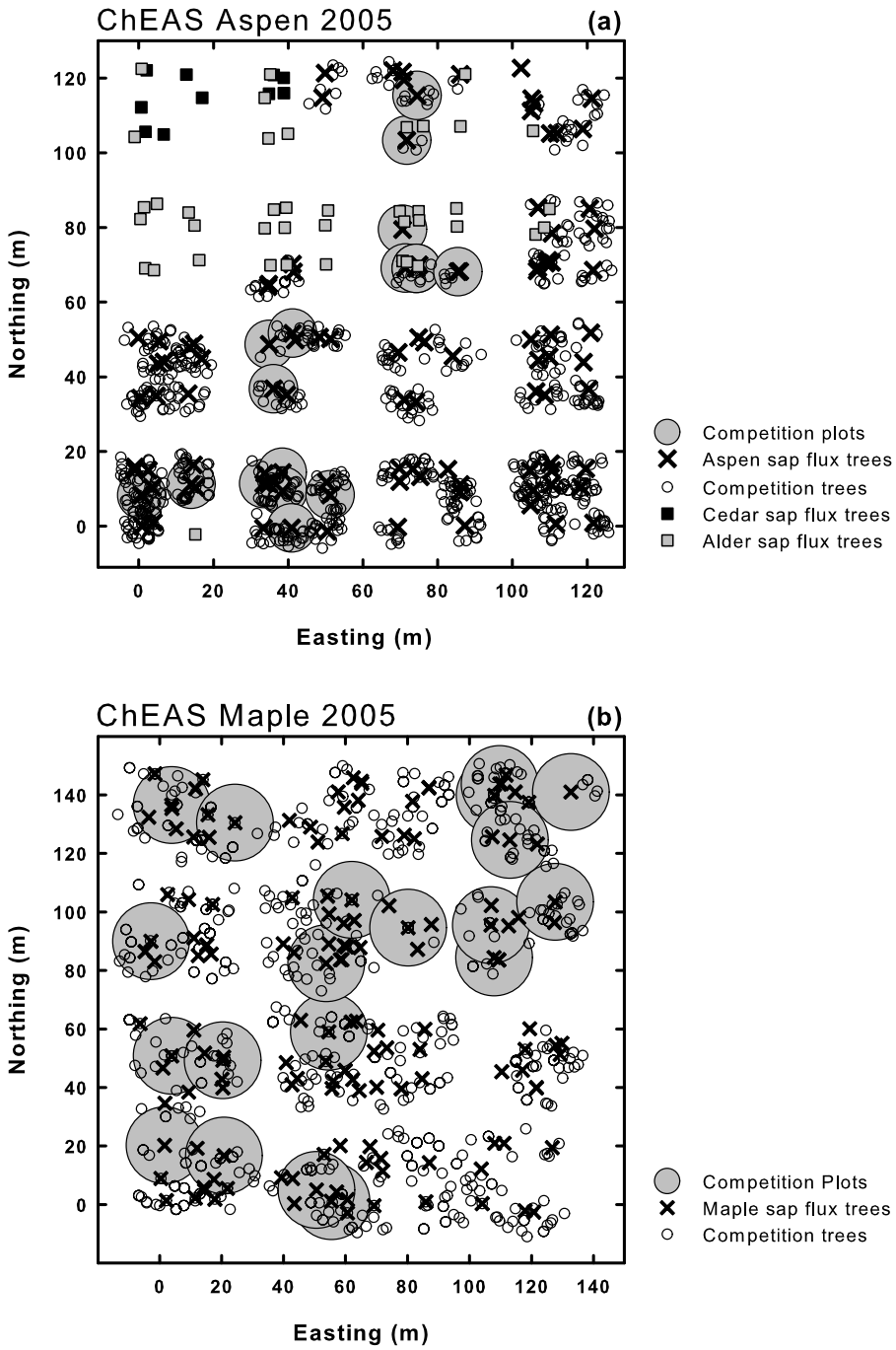

Figure 1. Map of (a) aspen and (b) maple sites. Large gray circles indicate 5 m and 10 m radius competition plots centered on the sap flux trees used for analysis in this study for aspen and maple, respectively. On both maps, crosses denote trees from the species used for analysis in this study instrumented for sap flux, and open circles represent trees sampled for sap flux only. The cyclic sampling design is reflected in the clustered location of (and subsequent gaps between) sap flux trees.

The second stand, referred to as maple, was dominated by mature sugar maple (*Acer saccharum* Marsh.) surrounding a large patch of plantation red pine (*Pinus resinosa* Ait.) with trees ranging in age from approximately 55–75 years. The portion of the site dominated by red pine comprised roughly 25% of the total area of the site in the form of an elongated area oriented in the northwest direction. The maple site was slightly larger measuring 132 m × 140 m and had approximately 15 m of variation in elevation across the site.

2.2. Data Collection

[10] A series of sample plots, measuring 5 m and 6.5 m in diameter at the aspen and maple sites, respectively, were established using a cyclic sampling design [*Burrows et al.*, 2002; *Clinger and Vanness*, 1976]. Initial site surveys revealed that tree size, indicated by diameter at breast height (*DBH*) varied across the site. Subsequently selecting the largest tree in each plot from the dominant species for sap

flux instrumentation yielded a representative sample [*Adelman et al.*, 2008; *Loranty et al.*, 2008]. For the aspen site the dominant species were aspen, alder, and cedar. At the maple site maple and red pine were the dominant species. In plots containing members of more than one of the dominant species one member of each species was selected for sampling, where resources allowed. Cyclic sampling is an efficient sampling method for geostatistical analysis, and a full description of the sampling and analyses at the aspen and maple sites is given by *Loranty et al.* [2008] and *Traver et al.* [2010], respectively.

[11] During the summer of 2005 approximately 300 trees were instrumented for sap flux measurements using the heat dissipation method [*Granier*, 1987]. Measurements at the aspen site began 27 May and ended 8 July. During the period from 15–20 June the site was shut down in order to recharge the power supply. Continuous measurements were made at the maple site from 19 July through 19 August. Sap flux data was processed using dynamic baselines to account for changes in sapwood moisture content and nighttime transpiration [*Oishi et al.*, 2008]. Point measurement of sap flux in the outer 20 mm of sapwood were scaled to the whole tree based on species specific radial trend measurements in sap flux and allometric relationships between sapwood depth and diameter measured ~10 km away in similar stands [*Ewers et al.*, 2002]. Estimates of observed E_C (mm s^{-1}, converted from g s^{-1}) were calculated from J_S measurements using the following equation:

$$E_{C-obs} = J_S \frac{A_S}{A_G} \tag{3}$$

where J_S is sap flux per unit xylem area (g m^{-2} s^{-1}) including species specific radial trend variation, A_S is sapwood area (m^2), A_G and is ground area (m^2). DBH was measured using a dendrometer band for each tree selected for sap flux instrumentation. Values of A_S were calculated from DBH using species specific allometric relationships established at nearby sites [*Ewers et al.*, 2002]. A_G was assumed to be the projected cross-sectional crown area for each individual. At the aspen site this was calculated from DBH using an allometric relationship developed with a subset cross-sectional crown area measurements made in conjunction with measurements taken to describe the competitive light environment within the canopy (described below). At the maple site the same approach was used, however the species specific allometric relationships used were taken from the literature [*Frelich and Lorimer*, 1985].

[12] Measurements of temperature and relative humidity (Vaisala HMP 45C, Vaisala Oyj, Helsinki, Finland) were made at two-thirds canopy height at both sites. Sap flux, temperature, and relative humidity measurements were recorded every 30 s (CR10X, Campbell Scientific, Logan, UT, USA) and aggregated to 30 min values. We measured volumetric surface (0–6 cm) soil moisture (Theta Probe, Delta-T, Cambridge, UK) in each plot on 30 May, 9, 13, 17, 22, and 25 June, and 12 and 14 July at the aspen site, and on 21 July at the Maple site. Values for each plot were determined by calculating the mean of three measurements taken at random locations within the plot. The soil moisture measurements were intended to represent the relative wetness of the plots rather than to serve as an indication absolute of root zone available moisture. Drought occurrence in these stands is rare [*Ewers et al.*, 2007a; *Mackay et al.*, 2002, 2007; *Samanta et al.*, 2008], and a piezometer installed at the aspen site supported this, as the water table remained <1 m from the surface near the edge of the wetland. Additionally obtaining root zone measurements for all 288 plots was not feasible.

[13] Several environmental variables required as model inputs including wind speed, Q_0, and precipitation (P) were acquired from the nearby WLEF (~2 km) [*Davis et al.*, 2003] and Lost Creek (~10 km) [*Cook et al.*, 2004] eddy covariance towers, respectively, depending on data availability and temporal resolution. *Ewers et al.* [2007a, 2008] have shown no difference between D measured at the WLEF tower and 2/3 canopy height from six stands in the region, indicating high canopy coupling. Leaf gas exchange measurements were made during the study period for a subset of trees at the aspen site. Scaffolding was erected over a period of several days and measurements of photosynthesis for sunlit and shaded leaves were obtained for approximately 6 aspen individuals in the upland portion of the site, and 6 individuals in the wetland portion of the site. Standard photosynthetic light response curves [*Long and Bernacchi*, 2003] were generated using observations made with an LI 6400 (Li-COR Biosciences, Lincoln, NE).

[14] In order to consider the potential effects of competitive shading we selected cloudless and cloudy days for data analysis because they are dominated by direct and diffuse radiation, respectively, and represent end-members of radiation conditions. Cloudless days were defined as days on which midday Q_0 was greater than 1800 μmol m^{-2} s^{-1} and diel plots of Q_0 exhibited minimal high-frequency variation indicative of partial cloud cover (Figures 2b and 2f). Cloudy days were defined as having relatively low Q_0, where ideally, midday values were in the range of 1000–1300 mmol m^{-2} s^{-1} and if possible no spikes exceeded 1500 mmol m^{-2} s^{-1} (Figures 2d and 2h). This measure was taken to ensure that individual values of G_{Sref} could be considered in the context of a tree's competitive light environment within the canopy, without the confounding effects of variation in Q_0 as a result of passing cloud cover, and then compared with values on cloudy days. Despite continuous monitoring, the extensive nature of the sites and the magnitude of upkeep required for sap flux sampling meant that days with site-wide data sets suitable for analysis were uncommon. Coincidentally large portions of both sites experienced power failures during the limited cloudless periods, and therefore a subset of approximately 20 trees from each site (Table 1) was selected for analysis based randomly on data availability related to the absence of power outages.

2.3. Stand Measurements

[15] Estimates of leaf area index (LAI) were required for the modeling portion of our study (described below). In order to ensure that modeled results were not artifacts of inaccurate canopy representation we calculated unique estimates of LAI for each individual tree used for analysis. An allometric equation relating LAI to DBH was developed via destructive harvest of 12 representative individuals across the stand. Such an approach was not feasible at the maple stand, and so we relied on regional allometric relationships taken from the literature [*Frelich and Lorimer*, 1985; *Perala and Alban*, 1994].

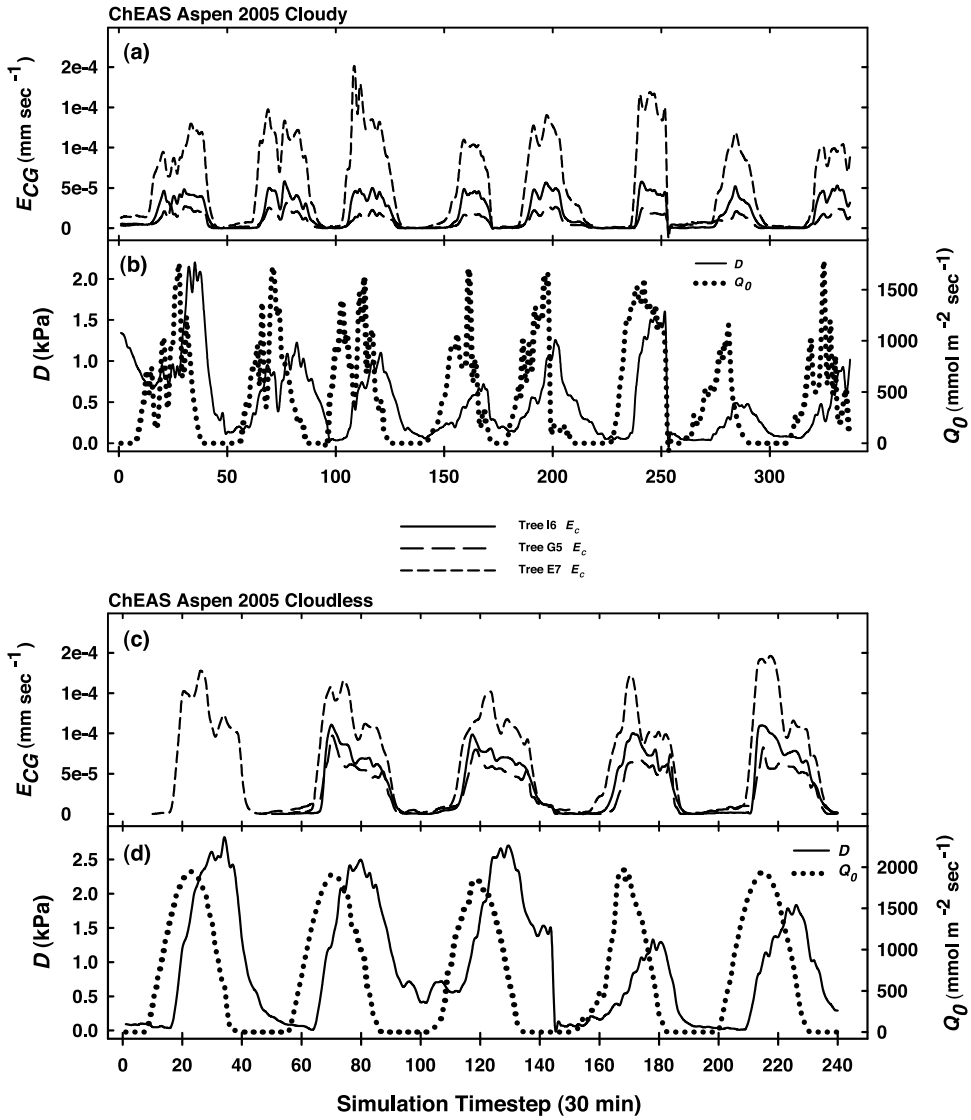

Figure 2. Diurnal trends of $E_{C\text{-}obs}$ from half-hourly sap flux data from three trees, and D and Q_0 for (a and b) cloudy and (c and d) cloudless at the aspen site, and (e and f) cloudy and (g and h) cloudless at the maple site.

[16] Distance-dependent measures of competitive crowding are commonly employed in ecological studies [*Bella*, 1971; *Berger and Hildenbrandt*, 2000; *Canham et al.*, 2004; *Lorimer*, 1983] including sap flux studies [*Lagergren and Lindroth*, 2004; *Phillips and Oren*, 1998]. To this end a series of measurements intended to describe the competitive light environment within the canopy were collected during August 2006 for the aspen site and August 2007 for the maple site. For each aspen and maple individual instrumented for sap flux an inventory was recorded of all neighbors within 5 m and 10 m, respectively. Distance and direction of each neighbor from the sap flux tree was recorded. Trees lying to the north of the sap flux tree between 345° and 45° were excluded on the grounds their competitive effects with respect to light within the canopy would be negligible. In addition tree heights for all trees were measured at the aspen site with triangulation methods using a laser rangefinder and clinometer. A combination of factors including a higher and denser canopy, a thick understory, and increased microtopography made height observation at the maple site impossible. As such tree heights at the maple stand were calculated using species-specific allometric equations developed for stands with similar structure and age within the region [*Frelich and Lorimer*, 1985; *Perala and Alban*, 1994]. At the maple site differences in relative tree height were determined using a LiDAR derived digital elevation model with 1 m resolution.

[17] Distance, direction, and height measurements for all competitors of an individual sap flux tree were used to calculate a competition index (C_I), which was defined as:

$$C_I = \sum_{i=1}^{n} \left(\frac{a_i}{180^\circ} \frac{1}{1+d_i} \frac{h_i}{h_s} \right) \tag{4}$$

where for each competitor i, a is the degree of southness to the sap flux tree when $a \leq 180^\circ$ and 1/2 azimuth direction where $a > 180^\circ$ (°), d_i is the distance between the sap flux

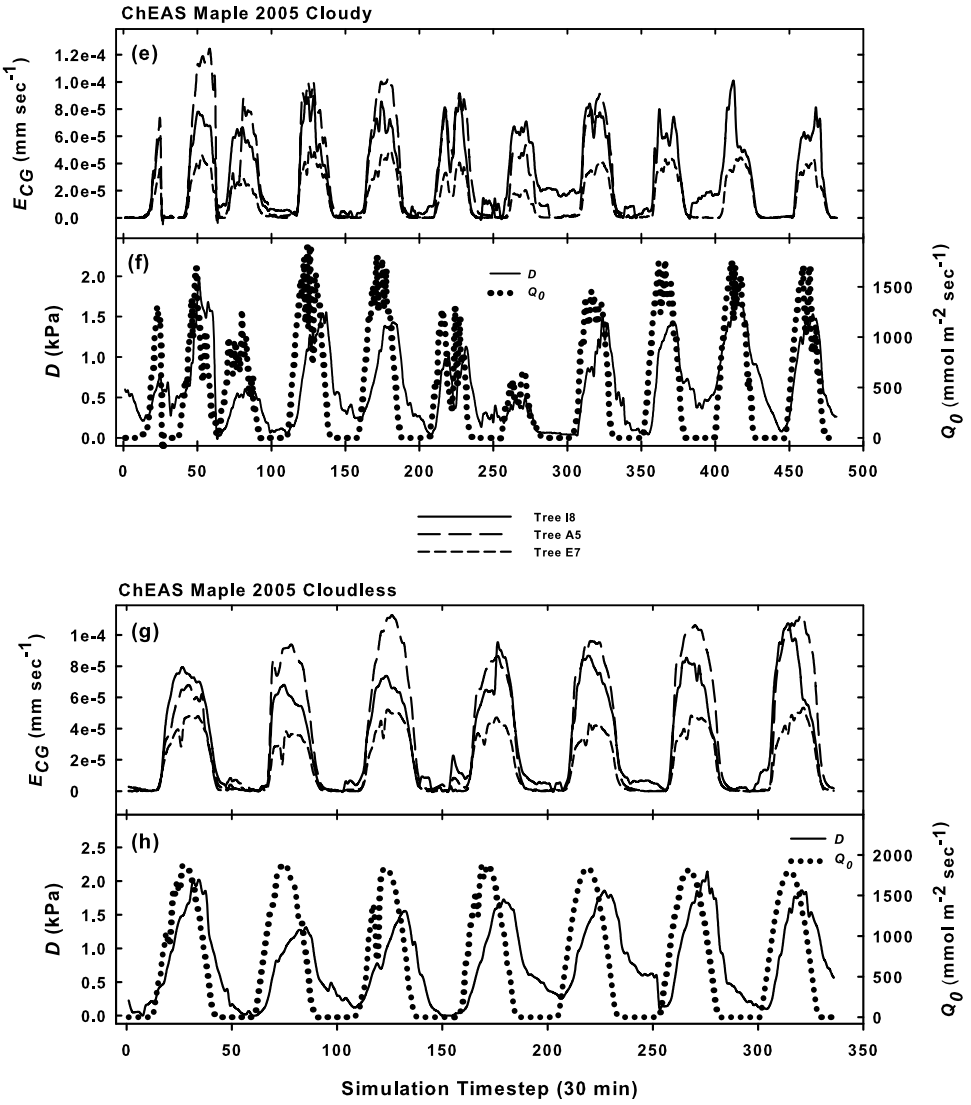

Figure 2. (continued)

tree and the competitor (m), h_s is the height of the sap flux tree, and h_i is the height of the competitor (m).

2.4. Model Description

[18] A brief overview of the Terrestrial Regional Ecosystem Exchange Simulator (TREES) [*Ewers et al.*, 2008; *Mackay et al.*, 2003; *Samanta et al.*, 2007, 2008] is provided in the following section, and more detail can be found in Appendix A. TREES is a canopy model that uses a modified big-leaf approach to simulate transpiration with a hybrid hydraulic and biochemical model of stomatal conductance [*Katul et al.*, 2000]. Light attenuation through the canopy for a given solar zenith angle, assuming a spherical leaf angle distribution and using a species-specific clumping parameter (Ω), is used to partition a given value of LAI into sunlit and shaded canopy elements. The model uses an initial hydraulic limited value of canopy stomatal conductance (G_{Sref0}), sampled at random from an uninformed distribution, which is constrained further using a photosynthesis model. This process is carried out in parallel for horizontal sunlit and shaded canopy layers. Final values of canopy stomatal conductance to water vapor are used to calculate transpiration for sunlit and shaded canopy elements individually, and then summed to yield simulated whole canopy transpiration ($E_{C\text{-}sim}$).

[19] In the model, photosynthesis (A_n) was calculated as described by *Farquhar et al.* [1980], and several parameters are required. Light acclimated quantum yield of photosynthesis (φ_J) expressed as mole electrons per mole of photons, is particularly important because it characterizes the response of A_n to Q_0 under low-light (light-limiting) conditions. This variable can be specified separately for sunlit and shaded canopy elements. At the aspen site in situ gas exchange measurements were collected and light response curves were constructed to determine φ_J. For the maple site gas exchange measurements from a nearby site were used. For both species no differences between sunlit and shaded

Table 1. Mean Values of Biometric Measurements for Individuals Sampled for Analyses, and Stand Inventories for Each Site[a]

Species	N[b]	DBH (cm)	H_T (m)	C_I	LAI[c] (m^2 m^{-2})	$Gsref$[d] (mmol m^{-2} s^{-1})	m (mmol m^{-2} s^{-1})
Aspen	18	8.1 (0.70)	10.0 (0.68)	1.43 (0.80)	4.06 (0.28)	73.0 (10.5)	42.7 (8.3)
	656	9.0 (0.13)	11.0 (0.11)	—	—	—	—
Maple	20	23.5 (1.5)	17.6 (0.52)	1.13 (0.75)	7.15 (0.53)	49.3 (3.8)	24.7 (4.2)
	454	22.1 (0.38)	16.4 (0.15)	—	—	—	—

[a]Mean G_{Sref} and m values are listed as well. Values in parentheses represent standard errors.
[b]Not all individuals selected were included for analyses based on model results.
[c]Only individuals with acceptable model results are included in parameter means.
[d]Site-wide mean LAI is not available because allometry for all species is not available.

leaves, or differences across edaphic conditions were observed. Values of 0.32 and 0.2 were used for aspen (this study) and maple (E. Kruger, unpublished data, 2010), respectively. Because $E_{C\text{-}sim}$ and G_{Sref} are modeled at the canopy scale accurate estimates of leaf area are essential for accurate estimates of fluxes and conductances. To achieve this we used unique estimates of LAI for each tree based on allometry described in section 2.3.

[20] For this study the model was run inversely using a Monte Carlo technique whereby multiple simulations are generated through repeated parameter sampling to yield a series of estimates of transpiration, which are subsequently evaluated against $E_{C\text{-}obs}$. Transpiration models calibrated using stand average $E_{C\text{-}obs}$ likely benefit from a reduction in signal noise resultant from data aggregation. Model calibration with data from individual trees should then be approached with this in mind. Here the parameters G_{Sref0} and m were allowed to vary to highlight differences in strategy for hydraulic regulation between individuals. An initial set of simulations were evaluated against an empirical estimate of stomatal conductance using only daytime observations and a fuzzy uncertainty approach [*Samanta and Mackay*, 2003] was used to constrain the range over which G_{Sref0} and m varied for each tree. A final set of simulations was generated using the constrained parameter ranges and then assessed by comparing $E_{C\text{-}sim}$ and $E_{C\text{-}obs}$. We found index of agreement (IOA):

$$IOA = 1 - \left(\frac{\sum_{i=1}^{n} (Obs_i - Sim_i)^2}{\sum_{i=1}^{n} \left(|Sim_i - Obs_i| + |Obs_i - \overline{Obs}| \right)^2} \right) \quad (5)$$

[*Willmott*, 1982] to be more robust than other fit statistics and so simulations were sorted by IOA in order identify the best model. Values of G_{Sref0} are initial estimates that may be further constrained by photosynthesis. Therefore we plotted simulated values of stomatal conductance (G_S) against D and fit a boundary line to the upper envelope of the curve by using the parameter m from the best model with equation (2), and adjusting G_{Sref} until the line passed through the upper envelope of the cloud of points (Figure 3).

2.5. Statistical Analysis

[21] A preliminary analysis revealed that where the highest $IOA < 0.80$ for a tree, there was typically a high degree of mismatch between simulated and observed data and a lack of convergence among parameter values (G_{Sref0} and m). Subsequently boundary lines formed using equation (2) did not pass through the upper envelope of the point cloud as expected (i.e., Figure 3), indicating that the parameters did not represent the data. Gaps in the data (i.e., partially missing days), erroneous data values, or a combination of both appeared to be the culprit. It is denoted in the results where $IOA < 0.80$ for an individual, and if this impacted the results parallel analysis with and without the data were conducted. Linear and nonlinear regression analyses were used to test for significant relationships ($p < 0.05$) between variables. All regression analyses were conducted with Sigmaplot (version 11.0 Systat Software, California, USA). Monte Carlo analyses and accompanying statistical evaluation of $E_{C\text{-}sim}$ and $E_{C\text{-obs}}$ were conducted using TREES, as described above.

3. Results

[22] Analysis of a preliminary set of simulations that were performed without the constrained parameterization technique described above yielded nearly identical results in terms of parameter values and goodness of fit (data not shown). The primary difference was a broader range of parameter values for the top models, some of which made little physiological sense (i.e., very low values of G_{Sref0} and high values of m) and made any analysis using only the top model questionable. Once the constrained parameterization

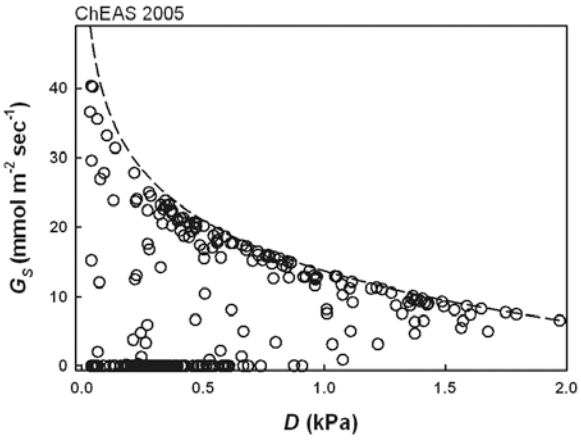

Figure 3. Boundary line fit to the upper envelope of G_S versus D used to determine G_{Sref}. The dashed curve represents the relationship $G_S = G_{Sref} - m\ln(D)$. The parameter value of m from the best model is used, and G_{Sref} is adjusted until the line to passes through the upper boundary of the point cloud. This allows G_{Sref} to be reduced relative to G_{Sref0} in the case that G_S has been reduced to account for light limitation. This process is repeated for each tree at both sites, under both light conditions.

Table 2. Summary of Model Parameterization Results for All Trees on Cloudless and Cloudy Days[a]

		Cloudless						Cloudy					
		IOA[b]		G_{Sref} (mmol m^{-2} s^{-1})		m (mmol m^{-2} s^{-1})		IOA[b]		G_{Sref} (mmol m^{-2} s^{-1})		m (mmol m^{-2} s^{-1})	
	Tree	Best	Mean	Best	Mean	Best	Mean	Best	Mean	Best	Mean	Best	Mean
A11	Aspen	0.84	0.83 (0.83–0.84)	87.0	90.0 (0.93)	60.0	61.0 (0.07)	0.72	0.72 (0.71–0.72)	92.0	74.4 (0.75)	60.2	62.2 (0.15)
C11	Aspen	0.92	0.91 (0.91–0.92)	105.0	111.6 (1.14)	86.9	89.4 (0.39)	0.83	0.83 (0.83–0.83)	150.0	156.2 (1.58)	118.0	119.2 (0.32)
D7	Aspen	0.92	0.92 (0.92–0.92)	155.2	154.3 (1.59)	105.3	107.0 (0.41)	0.93	0.93 (0.93–0.93)	175.0	213.8 (2.16)	116.3	115.9 (0.32)
D9	Aspen	0.84	0.83 (0.83–0.84)	46.0	46.8 (0.50)	26.0	27.8 (0.11)	0.76	0.76 (0.75–0.76)	42.0	42.7 (0.43)	28.0	30.0 (0.27)
D11	Aspen	0.83	0.83 (0.83–0.83)	33.7	34.4 (0.38)	20.1	21.2 (0.08)	0.72	0.70 (0.70–0.72)	27.0	27.8 (0.28)	20.4	22.4 (0.17)
D12	Aspen	0.88	0.87 (0.86–0.88)	37.0	47.5 (0.73)	10.2	47.5 (0.73)	0.85	0.83 (0.81–0.85)	31.5	36.9 (0.67)	10.2	36.9 (0.67)
E7	Aspen	0.92	0.92 (0.92–0.92)	162.0	161.0 (1.65)	116.8	117.2 (0.36)	0.92	0.92 (0.92–0.92)	152.0	174.6 (1.76)	121.3	122.6 (0.24)
E10	Aspen	0.89	0.89 (0.89–0.89)	45.9	47.2 (0.50)	22.1	23.5 (0.11)	0.70	0.69 (0.68–0.70)	28.5	34.4 (0.36)	22.3	23.8 (0.11)
E11	Aspen	0.86	0.86 (0.86–0.86)	41.0	42.3 (0.45)	20.1	21.0 (0.08)	0.81	0.81 (0.81–0.81)	36.5	37.3 (0.38)	21.4	23.3 (0.22)
E12	Aspen	0.83	0.83 (0.83–0.83)	52.3	53.7 (0.58)	24.0	25.3 (0.09)	0.72	0.72 (0.72–0.72)	42.5	42.7 (0.47)	24.0	25.3 (0.08)
F11	Aspen	0.89	0.89 (0.89–0.89)	50.1	50.1 (0.52)	19.2	20.1 (0.08)	0.75	0.75 (0.75–0.75)	40.0	41.5 (0.42)	19.2	21.6 (0.18)
G3	Aspen	0.67	0.67 (0.66–0.67)	22.0	22.6 (0.22)	11.0	11.2 (0.02)	0.80	0.80 (0.80–0.80)	23.0	22.6 (0.22)	11.0	11.3 (0.02)
G5	Aspen	0.90	0.90 (0.90–0.90)	105.0	107.1 (1.09)	42.7	44.4 (0.25)	0.80	0.79 (0.79–0.80)	57.5	60.5 (0.63)	41.0	43.5 (0.18)
G6	Aspen	0.87	0.87 (0.86–0.87)	33.0	35.1 (0.37)	11.0	11.5 (0.03)	0.70	0.69 (0.69–0.70)	24.5	25.6 (0.26)	11.1	12.0 (0.08)
H2	Aspen	0.79	0.78 (0.78–0.79)	30.0	34.4 (0.45)	10.0	11.6 (0.10)	0.68	0.66 (0.65–0.68)	30.0	17.5 (0.33)	10.1	11.2 (0.09)
H6	Aspen	0.81	0.80 (0.80–0.81)	27.6	28.3 (0.41)	15.0	15.9 (0.05)	0.67	0.66 (0.65–0.67)	30.0	27.3 (0.39)	15.0	16.3 (0.10)
H6-3	Aspen	0.94	0.94 (0.94–0.94)	73.0	81.5 (0.84)	43.1	45.5 (0.18)	0.81	0.80 (0.80–0.81)	71.0	73.3 (0.74)	44.0	48.4 (0.36)
I6	Aspen	0.91	0.91 (0.91–0.91)	95.0	108.0 (1.13)	70.0	70.4 (0.43)	0.84	0.83 (0.83–0.84)	130.0	94.4 (0.95)	68.7	74.4 (0.73)
A03	Maple	0.95	0.95 (0.95–0.95)	42.0	56.0 (0.65)	20.8	27.4 (0.53)	0.89	0.89 (0.89–0.89)	58.0	88.4 (0.90)	29.8	29.9 (0.31)
A05	Maple	0.96	0.96 (0.96–0.96)	61.0	71.0 (0.77)	28.6	30.0 (0.70)	0.87	0.87 (0.86–0.87)	80.0	105.4 (1.09)	18.2	21.7 (0.25)
A08	Maple	0.95	0.96 (0.91–0.96)	40.5	41.4 (0.61)	28.6	29.4 (1.14)	0.92	0.92 (0.92–0.92)	30.5	34.6 (0.36)	11.9	13.4 (0.17)
A12	Maple	0.98	0.98 (0.98–0.98)	49.5	55.4 (0.57)	18.3	19.2 (0.31)	0.91	0.91 (0.91–0.91)	54.5	63.1 (0.64)	41.7	41.2 (0.29)
C03	Maple	0.93	0.93 (0.92–0.93)	19.2	19.5 (0.24)	10.1	11.5 (0.09)	0.91	0.90 (0.89–0.91)	14.3	15.3 (0.22)	10.1	11.2 (0.08)
C05	Maple	0.89	0.94 (0.94–0.94)	52.7	50.4 (0.51)	76.5	27.1 (0.64)	0.95	0.95 (0.95–0.95)	46.5	47.2 (0.49)	31.0	47.2 (0.49)
C11	Maple	0.97	0.97 (0.97–0.97)	37.5	43.4 (0.44)	20.1	20.8 (0.19)	0.93	0.93 (0.93–0.93)	37.0	45.6 (0.46)	18.1	17.8 (0.15)
E01	Maple	0.98	0.98 (0.98–0.98)	40.0	42.7 (0.43)	21.9	21.6 (0.11)	0.93	0.93 (0.93–0.93)	38.0	45.3 (0.45)	15.3	15.7 (0.26)
E02	Maple	0.97	0.97 (0.97–0.97)	38.0	39.4 (0.40)	10.4	13.2 (0.20)	0.89	0.88 (0.88–0.89)	37.5	39.3 (0.40)	10.2	13.5 (0.24)
E06	Maple	0.95	0.95 (0.94–0.95)	68.5	71.1 (0.72)	14.3	18.3 (0.30)	0.92	0.92 (0.92–0.92)	65.0	71.7 (0.72)	55.9	53.8 (0.63)
E07	Maple	0.95	0.95 (0.95–0.95)	25.5	28.7 (0.31)	10.2	11.9 (0.11)	0.94	0.94 (0.94–0.94)	24.5	27.9 (0.30)	10.1	11.7 (0.12)
G09	Maple	0.95	0.95 (0.95–0.95)	50.0	54.2 (0.56)	26.3	27.3 (0.30)	0.93	0.93 (0.93–0.93)	54.5	63.2 (0.64)	47.1	47.9 (0.34)
I08	Maple	0.94	0.94 (0.94–0.94)	35.0	46.3 (0.50)	14.3	17.3 (0.34)	0.89	0.89 (0.89–0.89)	49.5	61.0 (0.63)	52.7	52.9 (0.40)
J07	Maple	0.92	0.92 (0.92–0.92)	52.7	52.2 (0.54)	40.9	41.4 (0.27)	0.90	0.90 (0.90–0.90)	53.0	64.7 (0.65)	46.9	47.8 (0.41)
J08	Maple	0.92	0.92 (0.92–0.92)	79.0	91.5 (0.95)	74.0	76.1 (0.47)	0.92	0.91 (0.91–0.92)	65.0	126.8 (1.80)	122.3	125.9 (1.56)
J11	Maple	0.95	0.95 (0.95–0.95)	33.0	35.9 (0.39)	19.9	19.6 (0.29)	0.80	0.80 (0.80–0.80)	15.5	15.4 (0.17)	28.2	28.8 (0.26)
J12	Maple	0.95	0.95 (0.95–0.95)	35.5	39.8 (0.41)	17.1	17.5 (0.23)	0.85	0.85 (0.84–0.85)	50.0	57.5 (0.58)	10.2	14.1 (0.28)
K10	Maple	0.95	0.95 (0.95–0.95)	32.5	37.2 (0.42)	14.0	15.3 (0.36)	0.93	0.93 (0.92–0.93)	75.0	41.3 (0.48)	10.0	12.4 (0.16)
L09	Maple	0.96	0.96 (0.96–0.96)	29.5	36.2 (0.38)	16.0	17.4 (0.08)	0.95	0.95 (0.95–0.95)	25.0	41.4 (0.44)	16.1	16.9 (0.06)
L12	Maple	0.96	0.96 (0.96–0.96)	60.0	74.2 (0.77)	11.1	16.3 (0.34)	0.93	0.93 (0.93–0.93)	67.5	80.9 (0.83)	53.0	54.0 (0.45)

[a]Values of IOA, G_{Sref}, and m for the best fit model are compared with mean values from the top 100 models to illustrate model convergence. The range of mean IOA values is indicated in parentheses, and standard error of the mean is in parentheses for mean G and m.

[b]Values in parentheses indicate the range of IOA values for the top 100 models.

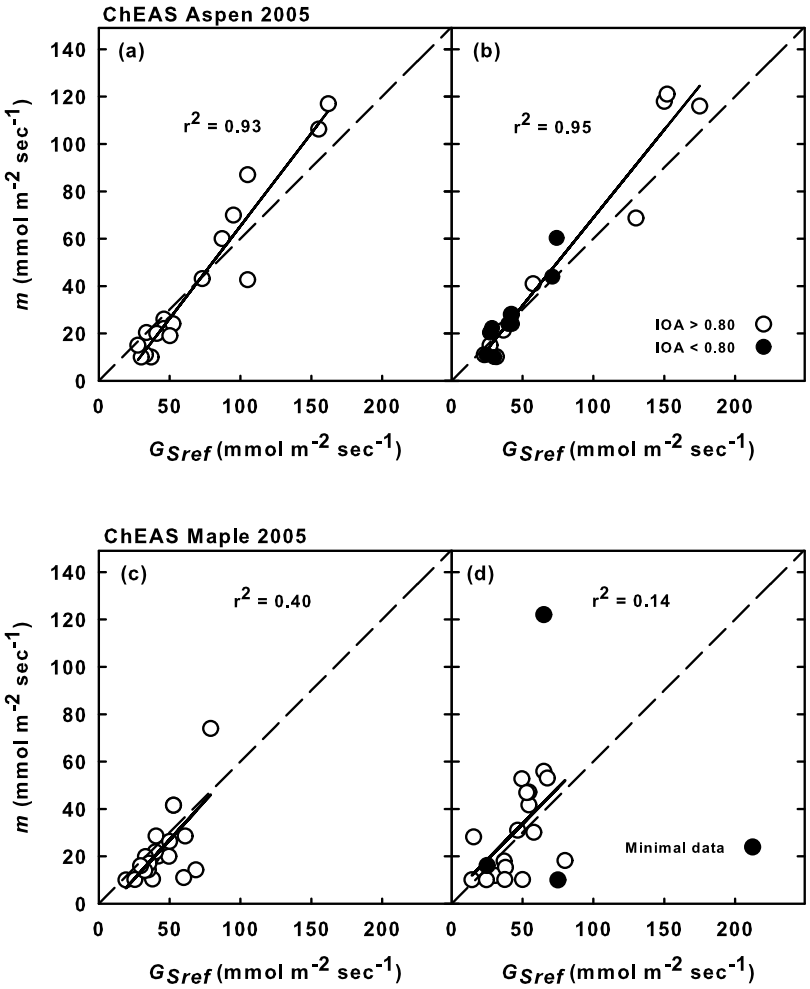

Figure 4. G_{Sref} plotted against m for aspen on (a) cloudless and (b) cloudy days, and maple on (c) cloudless and (d) cloudy days. Open circles represent acceptable models, and solid circles represent models with $IOA < 0.80$. The dashed line represents $m = 0.6G_{Sref}$ after equation (2), and solid lines are linear regressions.

was applied the model converged on a narrow range yielding a much more robust set of parameter values for each tree that are essentially identical for the best fitting models (Table 2).

[23] Simulations with TREES achieved varied results across the range of conditions and species (Table 2). In general the model performed better on cloudless days when $E_{C\text{-}obs}$ was high and limiting drivers exhibited consistent diurnal trends (Figure 2). Simulated transpiration showed highest agreement with observations from the maple site taken on sunny days, with IOA values between 0.92 and 0.98. At the aspen site values of IOA ranged from 0.58 to 0.92 for simulations parameterized against the cloudless data subset. On cloudy days when D and Q_0 were low and exhibited more variability, there was less agreement between $E_{C\text{-}sim}$ and $E_{C\text{-}obs}$. Values of IOA ranged from 0.80 to 0.95, and 0.67 to 0.93 for simulations parameterized against data from the cloudy subset for maple and aspen, respectively.

[24] Values of G_{Sref} derived from boundary line analyses were compared to the parameter m generated using TREES (Figure 4). Models showed good agreement with the expected 0.6 proportionality between m and G_{Sref}, with individuals at the maple site showing slightly more deviation during both cloudless and cloudy days. Comparison of G_{Sref} within species for cloudless and cloudy days revealed little variation (Figure 5). In light of this relative invariance in G_{Sref} between light conditions (cloudy or cloudless), subsequent analyses utilizing G_{Sref} were conducted utilizing both separately and with a combined cloudless and cloudy data set, and the combined analyses is presented in cases where cloudless and cloudy results are consistent.

[25] Topoedaphic position, as indicated by surface soil moisture, appears to exert little or no influence on G_{Sref} for either site. At the maple site there was minimal variability in soil moisture and subsequently no relationship between G_{Sref} and soil moisture ($r^2 = 0.0$, $p > 0.05$) (Figure 6). Despite a pronounced soil moisture gradient at the aspen site no relationship was observed between G_{Sref} and soil moisture ($r^2 = 0.0$, $p > 0.05$) (Figure 6).

[26] In order to test the hypothesis that competition for light contributes to variability in G_{Sref} we simulated the effects of reduced light using the model (Figure 7), and compared G_{Sref} to C_I and its component variables. Inverse relationships were observed between G_{Sref} and C_I for both aspen and maple under both light conditions. At the maple

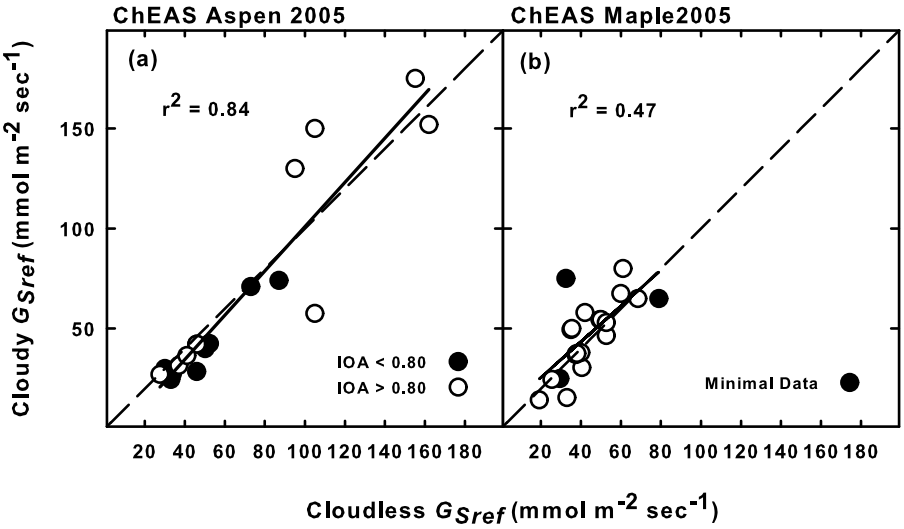

Figure 5. G_{Sref} from cloudy days plotted against G_{Sref} from cloudless days for (a) aspen and (b) maple. Open circles represent acceptable models. Solid circles represent models with $IOA < 0.80$ for aspen (Figure 5a), and trees with less than 2 full days worth of data for maple (Figure 5b). Dashed lines denote a 1:1 relationship, and solid lines are linear regressions.

site a linear regression revealed a significant relationship between G_{Sref} and C_I ($r^2 = 0.32$, $p < 0.001$). At the aspen site a significant nonlinear relationship was found between G_{Sref} and C_I ($r^2 = 0.36$, $p < 0.01$) (Figure 8). Excluding cloudy data from this analysis improved the relationship with the same nonlinear model ($r^2 = 0.50$, $p < 0.01$). To test the idea that the relationship between G_{Sref} and C_I was indicative of competitive shading we selected two individuals from the aspen site with poor *IOA* values on cloudy days (A11, H6). A simple uniform reduction in radiation was achieved by reducing observed Q_0 by 50%. We then used otherwise identical methodology to generate a new set of 10,000 simulations for each tree. In both cases IOA for the best model increased substantially, yielding fits acceptable for analysis ($IOA > 0.80$) (Figure 7).

[27] A weak positive correlation was observed between G_{Sref} and A_S at both sites for cloudless and cloudy days combined, this correlation was statistically significant at the aspen site ($r^2 = 0.58$, $p < 0.001$) but not at the maple site ($r^2 = 0.06$, $p > 0.05$) (Figure 8). Similarly, weak nonsignificant ($r^2 = 0.12$, $r^2 = 0.0$, $p > 0.05$) correlations between G_{Sref} and H_T were observed for both aspen and maple sites, respectively. Additional analyses were conducted with each individual distance, direction, and height component of C_I ($p > 0.05$). Excluding each component of C_I for maple similarly degraded the relationship between it and G_{Sref}, suggesting an equal contribution to C_I. For aspen the direction of competitors appeared to have little or no influence on G_{Sref}, and excluding it from C_I had negligible impacts on the relationship between G_{Sref} and C_I. A stepwise

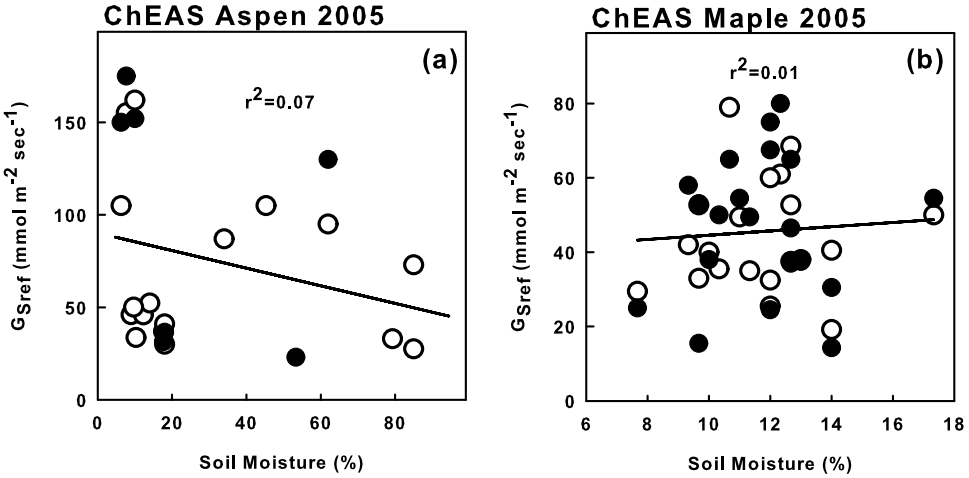

Figure 6. G_{Sref} plotted against surface soil moisture for (a) aspen and (b) maple sites. Volumetric soil moisture measurements for each site were obtained for the top 6 cm of soil and are intended to be a proxy for topoedaphic positions rather than an indication of absolute available root zone soil moisture. Linear regressions are shown as solid lines.

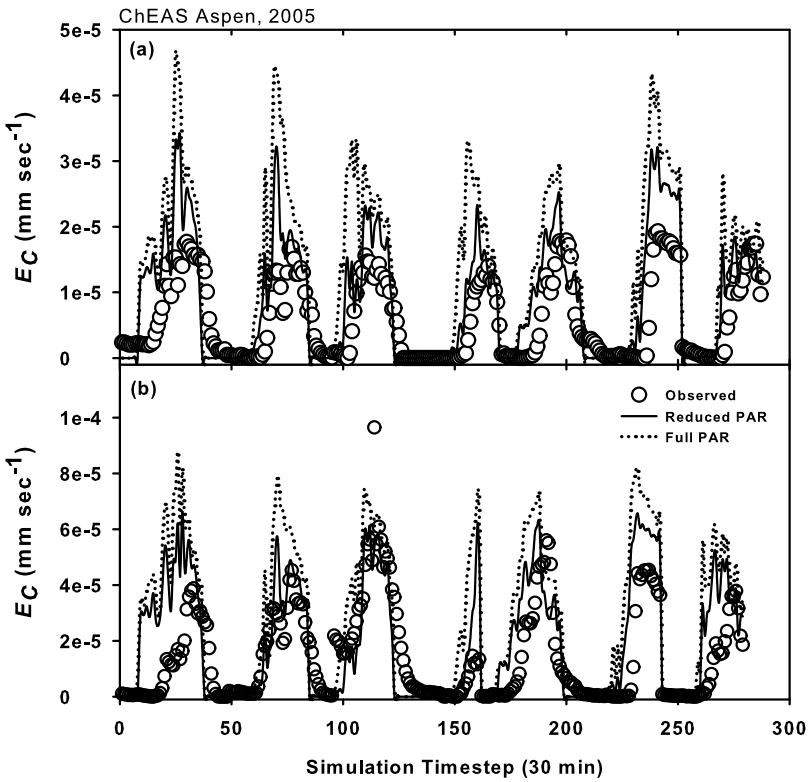

Figure 7. Plots of E_C for aspen trees (a) H6 and (b) A11. Simulations generated using full Q_0 and Q_0 reduced by 50% are compared to observations. These trees were selected for reanalysis based on their originally low values of *IOA*, in order to test the hypothesis that competition for light affects G_{Sref} and that not accounting for competitive shading may be a cause for poor model performance.

regression was conducted between G_{Sref} and C_I, A_S, H_T, and soil moisture, and no significant correlation between variables was revealed ($p > 0.05$).

4. Discussion

[28] Our results show within species variability in G_{Sref} for aspen and maple, and this finding supports the first hypothesis that G_{Sref} is heterogeneous at the stand scale. For both species we observed a linear relationship between G_{Sref} and m, a finding that supports our second hypothesis. This result is not particularly unexpected, but there have been few studies with adequate data to address questions regarding intraspecies variability in G_{Sref} and so it has not been explicitly tested. The relationship between G_{Sref} and C_I supports our third hypothesis that competition for light contributes to variability in G_{Sref}.

4.1. Model Evaluation

[29] Simulated transpiration showed good overall agreement with our observations, and there are several points to be considered when evaluating model performance and results. Ecosystem models such as TREES are typically parameterized and evaluated with stand-scale flux observations utilizing either aggregated sap flux or tower based eddy covariance data [*Kuchment and Demidov*, 2006; *Raulier et al.*, 2002; *Stoy et al.*, 2006; *Wang et al.*, 2007]. In this context, aggregated flux estimates benefit from data smoothing, and subsequently a relatively high degree of agreement between simulations and observations can often be achieved. On the other hand, the relatively low signal-to-noise ratio of sap flux observations [*Oren et al.*, 1998] for individual stems can make parameterization more difficult.

[30] Diurnal plots of sap flux data for individual aspen stems generally exhibit a relatively high degree of micro-scale temporal variability (i.e., lack of smoothing), particularly in comparison to maple (i.e., Figures 2a and 2c versus Figures 2d and 2f). So, while simulated transpiration values for both species may accurately capture the diel response of whole plant water use to D, variability at small timescales for aspen, typically during midday, result in lower *IOA* between simulated and observed values (Table 2). A likely explanation is that aspen sap flux exhibits a much more dynamic response to environmental drivers because of its relatively small size and high water use [*Ewers et al.*, 2002, 2005, 2007a]. *Ewers and Oren* [2000] report increased variability between consecutive measurements with a decrease in storage capacity. More recently, *Burgess and Dawson* [2008] have cautioned against using continuous heat sensors for inferring capacitance because of lags associated with heat buildup in the xylem tissue surrounding the sensors. In contrast *Ewers et al.* [2007b] observed no lags between water fluxes measured in stems using continuous heat sensors (Granier) and branch fluxes measured using compensating heat sensors (Kucera), and similar results are described in a recent review by *Phillips et al.* [2009]. Both of these studies report higher fluxes in illuminated branches than shaded ones. Thus it is reasonable to expect more variability at half-hourly time steps for aspen because they have smaller stems.

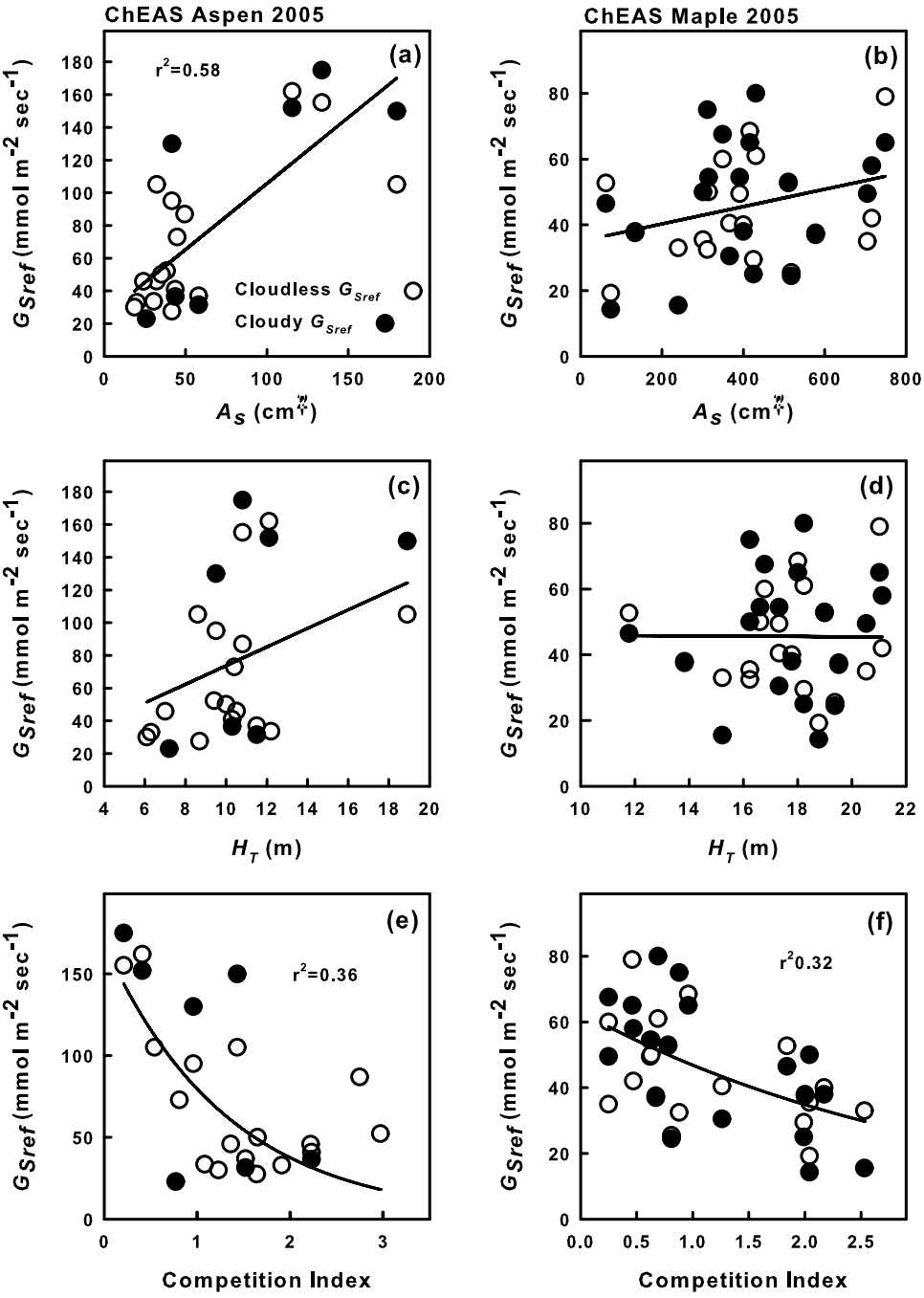

Figure 8. G_{Sref} plotted against (a and b) A_S, (c and d) H_T, and (e and f) CI for aspen and maple, respectively. Lines represent regressions, and r^2 values are shown. Significant relationships were observed between G_{Sref} and A_S ($r^2 = 0.58$, $p < 0.01$) for aspen, and G_{Sref} and C_I for both aspen and maple ($r^2 = 0.36$, $p < 0.1$, and $r^2 = 0.31$, $p < 0.01$), respectively.

4.2. Non-Light-Limiting Effects

[31] No significant relationship between G_{Sref} and soil moisture was observed at either site, and this is consistent with findings from other studies in the region [*Ewers et al.*, 2002, 2007a, 2008; *Samanta et al.*, 2008]. At a variety of scales an inverse relationship has been observed between soil water potential and G_S (and subsequently J_S, and $E_{C\text{-}obs}$) [*Aranda et al.*, 2005; *Cochard et al.*, 2002], and so an increase in G_{Sref} with soil moisture could be expected. At the aspen site water table height, observed using a pair of soil water wells in the wetland portion of the site, was never further than 1 m from the soil surface (data not shown). This suggests an absence of drought stress [*Mackay et al.*, 2003], less heterogeneity in soil moisture with depth, and unlikely occurrence of upland drought stress. Alternatively, near saturated soils in the wetland portion of the site may have been detrimental to aspen, an assertion supported by their relative lack of abundance and small size there [*Traver et al.*, 2010]. A concurrent study by *Traver et al.* [2010]

found no significant correlations between soil texture, moisture, bulk density, nitrogen content, or C:N and within species J_S, $E_{C\text{-}obs}$, or E_L at either site.

[32] Numerous studies have explored relationships between stomatal conductance and biometric variables related to tree size and age such as A_S [*Moore et al.*, 2004], H_T [*Franks*, 2004; *Novick et al.*, 2009; *Schafer et al.*, 2000; *Woodruff et al.*, 2007], and A_S:A_L [*McDowell et al.*, 2002]. Increases in A_S and height with age are typically accompanied by an increase in A_S:A_L and subsequently whole canopy stomatal conductance. This can be attributed to increases in resistance along the hydraulic pathway from the soil to the atmosphere. This type of hydraulic limitation typically occurs in trees much taller than the ones at our sites. An inverse relationship between H_T and G_{Sref} has been observed [*Novick et al.*, 2009; *Schafer et al.*, 2000]; however, the range of H_T in our study was small relative to the range of G_{Sref} values. Additionally, H_T was used as a proxy for emergence. Absence of a strong relationship between G_{Sref}, and A_S, or H_T suggests additional information regarding ecosystem structure is necessary to elucidate apparent differences in G_{Sref} between individuals for the species in question, although the use of allometry to obtain H_T for maple may introduce variability (i.e., Figures 8d and 8f).

[33] Correlation between G_{Sref} and C_I (Figure 8) implicates stand structure as a factor that contributes to variation in hydraulic regulation between individuals. One possibility is that stem density serves as a proxy for water and nutrient demand in the soil. Increased root density could place greater demand on the supply of available water and nutrients. Lower ψ_S as a consequence of increased demand would lower stomatal conductance (equation (1)). Reduced N availability may potentially lower photosynthetic capacity and G_S in turn. However, no relationship was found between G_{Sref} and stem density alone (data not shown).

4.3. Light-Limiting Effects

[34] We suggest competition for light between canopies as an explanation for variable G_{Sref}. A known relationship exists between solar irradiance and photosynthetic rates [*Walcroft et al.*, 2002], and increased transpiration has also been observed in illuminated branches [*Burgess and Dawson*, 2008; *Ewers et al.*, 2007b]. Functional differences between sunlit and shaded leaves, typically found in the upper and lower portion of canopies, respectively, have also been observed [*Naidu and Delucia*, 1997]. The light environment in which leaf development occurs has been shown to affect leaf photosynthetic capacity, i.e., individuals that develop in shade have lower capacity for photosynthesis [*Lei and Lechowicz*, 1997; *Niinemets et al.*, 2004]. Although observation have been observed in seedlings and saplings, similar affects manifested in biomass allocation (leaf mass per unit area) have been observed in mature trees [*Jones and Thomas*, 2007]. As such a reasonable hypothesis is that trees at a competitive disadvantage to their neighbors with respect to canopy light environment may have a higher proportion of shaded leaves and subsequently light-limited photosynthesis that would in turn limit stomatal conductance. For these trees it would not be beneficial to have high G_S during periods of low D and Q_0 (i.e., high G_{Sref}) because water loss would be disproportionately large in comparison to carbon gain due to light limitation. Conversely for emergent trees with little competition and relatively little light limitation a more economical approach would be to maximize productivity with readily available light before hydraulic limitation forces stomatal closure.

[35] Our finding that a simple light reduction improves *IOA* for two aspen individuals (Figure 7) supports the assertion that competition for light may explain variability in G_{Sref}. This light reduction was intended to represent a shift of the crown from an emergent position in the canopy to a "submergent" one. As such a decrease in incident radiation without concurrent changes in other microclimate variables can be assumed. It has been shown that changes in soil temperature and moisture across understory light gradients are negligible [*Porté et al.*, 2004] and even in canopy gaps understory vegetation has been shown to exert more control on such variables than overstory absence [*Clinton*, 2003]. Additionally previous studies in this region have shown D to be well mixed throughout canopies over a range of conditions [*Ewers et al.*, 2007a, 2008]. This information in combination with prior findings that exhibit the lack of a clear relationship between G_{Sref} and other edaphic variables that related to competition in general indicate that C_I is a suitable proxy for competition for light despite a lack of explicit light measurements.

[36] Simulations for certain individuals at the aspen site may be interpreted in the context of light limited stomatal conductance. The model was achieved good agreement with data from aspen trees E7 and D7, two individuals with very low values of C_I values of 0.41 and 0.21, respectively. Effectively these trees were in the open, as they grew on the north edge of a large gap, created by a series of blow-downs preceding the study period. Subsequently these trees also have among the highest G_{Sref} values at the site (Figure 8). One possible explanation is that individuals such as these with minimal light limitation exhibit higher G_{Sref} in order to maximize carbon gain before the onset of hydraulic limitation by D, whereas trees subject to competitive shading would be light limited and therefore not benefit from high G_{Sref}. For reference tree E7 is located at (41°E, 50°N) in Figure 1a, and transpiration data are shown in Figures 2a and 2c.

[37] TREES accounts for self-shading within a bulk canopy and so it is likely that inaccuracies exist in estimates the proportions of absorbed direct and diffuse radiation that are manifested in G_{Sref} estimates. For bulk canopies this may be appropriate, but when applied to a single crown this means that sunlit and shaded canopy elements are derived as a function of light attenuation through the crown itself with no consideration for the effects of horizontal or vertical heterogeneity (i.e., neighboring trees). As a result it is probable that the model does not capture spatial variability in light limited photosynthesis as a consequence of canopy structural heterogeneity. In cases where photosynthesis is light-limited and stomatal conductance is affected overall model performance would be improved, as evidenced in Figure 7. Our results suggest most trees receive sufficient radiation for maximum photosynthesis on cloudless days, and that only trees with high C_I are light limited on cloudy days (as evidenced, for example, by decreased *IOA* on cloudy days at the aspen site). This indicates that trees overestimates incident radiation for cloudy days. Incorporating spatial variability in incident radiation into TREES through three-dimensional radiative transfer modeling may

offer a clearer mechanistic explanation [*Chen et al.*, 2008; *Courbaud*, 2003; *Lappi and Stenberg*, 1998; *Larocque*, 2002].

5. Conclusions

[38] We have employed a simple ecosystem model that utilizes hydraulic and photosynthetic constraints to illustrate that stomatal conductance exhibits within species variability across two forested stands in northern Wisconsin. Individuals for both species remained isohydric, exhibiting a linear relationship between reference stomatal conductance and sensitivity to atmospheric vapor pressure deficit, and these results were consistent with cloudless and cloudy days for both sites. Analysis of a series of environmental and biological factors indicates that a competition index, designed to characterize competition for light as a results of canopy structural heterogeneity, is most strongly related to spatial variability in stomatal conductance for both sites. On cloudy days at the aspen site the model generally over predicted transpiration resulting in poor agreement between simulated and observed data. Two trees with relatively low C_I values are of notable exception. It is suggested that variability in photosynthetic light limitation as a result of competitive shading offers a mechanistic explanation for this finding. Furthermore absence of clear physiological differences between sunlit and shaded leaves within species indicates a dynamic stomatal response to light environment rather than long-term physiological acclimation.

[39] Our results suggest that forest stand structure should be considered when generating estimates of stomatal conductance for use in hydrologic models, particularly where structural heterogeneity is high. With regards to stand and regional scale estimates of water fluxes these results are in line with results of previous studies from these sites in that they highlight the need for thoughtful plot location of point measurements, but do not negate the current point-to-area scaling method. Additionally the apparent link between stomatal conductance and ecosystem structure suggests that high-resolution remote sensing can be utilized to identify areas with high variability in ecosystem fluxes where representative sampling is imperative for accurate upscaling. Future research should seek to further elucidate the effects of variable incident radiation on stomatal control of transpiration in order to better understand temporal changes in spatial variability that occur on diurnal timescales.

Appendix A

A1. Model Description

[40] TREES was initialized with an approximation of stomatal conductance (G_{S0}) (mmol m^{-2} s^{-1}) limited by hydraulics using equation (2) where parameter values of reference stomatal conductance (G_{Sref0}) and m were sampled at random. For each canopy element (k) leaf specific CO_2 conductances ($g_{c0,k}$) were calculated using the following equation:

$$g_{c0,k} = \frac{1}{\frac{1}{G_{S0}L_K} + \frac{1}{g_{va}}} \frac{1}{L_k} \frac{1}{1.6} \tag{A1}$$

where L_k is element leaf area index (m^2 m^{-2}), g_{va} is aerodynamic conductance which is a function of turbulent and laminar heat and vapor conductance (mmol m^{-2} s^{-1}), and 1.6 is the proportionality between molar H_2O and molar CO_2. These values of hydraulically constrained stomatal conductance to CO_2 were subsequently used to calculate photosynthesis using a hybridization of models described by *Katul et al.* [2000, 2003], and *de Pury and Farquhar* [1997], that allows for electron transport (light) limited and Rubisco (nitrogen) limited photosynthesis. The results of this model were used to calculate stomatal conductance to H_2O for each canopy element ($g_{v,k}$):

$$g_{v,k} = 1.6 \frac{A_{n,k}}{c_a - c_{i,k}} \tag{A2}$$

where A_n is net photosynthesis (μmol m^{-2} s^{-1}), c_a is atmospheric CO_2 concentration (Pa), and c_i is intercellular CO_2 concentration (Pa). This relationship assumes atmospheric CO_2 and leaf surface CO_2 concentrations to be equivalent. At this point canopy element transpiration was calculated using the Penman-Monteith Combination Equation [*Monteith*, 1965]:

$$E_{C,k} = \lambda^{-1} \frac{sR_{n,k} + \gamma_k^* \lambda g_{v,k} \frac{D}{p_a}}{s + \gamma_k^*} \tag{A3}$$

where λ is the latent heat of vaporization (J kg^{-1}), s is the slope of the saturation vapor pressure temperature curve (mbar $°C^{-1}$), R_n is net radiation (W m^{-2}), γ^* is the modified apparent psychrometric constant (mbar $°C^{-1}$), and p_a is the density of air (kg m^{-3}). Values of transpiration for each canopy element are then summed to yield total canopy transpiration.

[41] As previously mentioned the above calculations are conducted in parallel for sunlit and shaded canopy elements. Sunlit leaf area of the canopy (L^*), as described by *Campbell and Norman* [1998], is defined as:

$$L^* = \frac{1 - \exp(-K_{be}(\Psi)L)}{K_{be}(\Psi)} \tag{A4}$$

where L is leaf area index (m^2 m^{-2}), and $K_{be}(\Psi)$ is the extinction coefficient for light in the canopy at zenith angle Ψ, based upon an ellipsoidal leaf angle distribution. The shaded portion of the canopy is then calculated by subtracting L^* from L. $K_{be}(\Psi)$ is calculated as follows:

$$K_{be}(\Psi) = \frac{\sqrt{x^2 \tan^2 \Psi}}{x + 1.774(x + 1.182)^{-0.733}} \Omega(\Psi) \tag{A5}$$

where x is the leaf angle distribution, and $\Omega(\psi)$ is a canopy clumping parameter ranging from 0 to 1 that varies with zenith angle according to the following equation:

$$\Omega(\Psi) = \frac{\Omega}{\Omega + (1 - \Omega)\exp(-2.2(\Psi)^p)} \tag{A6}$$

where Ω is the clumping parameter when the canopy is viewed from nadir, and p is a variable related to the ratio of crown height to crown diameter. Typically x, Ω, and p are species-specific model input parameters derived from liter-

ature values [*Campbell and Norman*, 1998]. Incident radiation is partitioned into direct and diffuse components according to *Spitters et al.* [1986].

A2. Model Parameterization

[42] To assure adequate parameterization with respect to G_{Sref0}, we ran a preliminary set of 10,000 simulations for each tree under cloudless conditions. Parameter values for G_{Sref0} and m were allowed to vary over a range that was based on previous measurements of these species near the current stands [*Ewers et al.*, 2007a]. The preliminary analysis evaluated simulated G_S against empirically derived values of G_S during hours of peak E_C (approximately 1000–1600 local standard time), when stomatal limitation was apparent. We calculated G_S using the following empirical equation derived by inverting the Penman-Monteith equation [*Monteith and Unsworth*, 1990] and assuming high canopy coupling:

$$G_S = \frac{K_G T E_L}{D} \tag{A7}$$

where K_G [*Phillips and Oren*, 1998] is the conductance coefficient ($115.8 + 0.4236T$) that accounts for the latent heat of vaporization, temperature effects on the psychrometric constant, the density of air, and the specific heat of air at constant pressure (kPa m^3 kg^{-1}), and E_L is transpiration per unit leaf area (m s^{-1}). Following the method of *Samanta and Mackay* [2003] each of the 10,000 models from a set of simulations was assigned a membership grade based on a series of goodness-of-fit measures, and a subset of acceptable models was treated as a fuzzy set with inherent uncertainty [*Ewers et al.*, 2008; *Mackay et al.*, 2003]. An alpha cut is assigned and used to determine the cardinality of the subset of acceptable models and this in turn is used to determine the cardinality for a crisp set. From this crisp set the range of parameter values for the G_{Sref0} and m was then used to constrain the range of parameters for the second set of simulations. Using the constrained ranges of possible parameter values a further 10,000 simulations were generated for each tree, under both cloudless and cloudy conditions. For this second set of simulations the models were evaluated against values of $E_{C\text{-}obs}$ over entire days.

[43] As described above, parameter values for G_{Sref0} are initial estimates that may be further constrained by photosynthesis. Therefore we plotted simulated values of stomatal conductance (G_S) against D and fit a boundary line to the upper envelope of the curve by using the parameter m from the best model with equation (2), and adjusting G_{Sref} until the line passed through the upper envelope of the cloud of points (Figure 3). G_S was calculated as:

$$G_S = \frac{\left(g_{v,sun} - \frac{g_{va}}{L_{sun}}\right) L_{sun} + \left(g_{v,shd} - \frac{g_{va}}{L_{shd}}\right) L_{shd}}{L} \tag{A8}$$

where g_{vsun} and g_{vshd} are stomatal conductance for sunlit and shaded canopy elements, respectively (equation (A2)) (mmol m^{-2} s^{-1}), g_{va} is bulk aerodynamic conductance (mmol m^{-2} s^{-1}), and L is leaf area index. L_{sun} and L_{shd} are sunlit and shaded leaf area index (m^2 m^{-2}). This process was performed for the top simulation for each tree under both cloudless and cloudy conditions, and the resulting values of G_{Sref} and m were used for analysis. Using simulated values of G_S to calculate G_{Sref} is beneficial because it removes the effects of g_{va}, which is not the case for empirical approaches.

[44] **Acknowledgments.** Funding for this study was from the National Science Foundation, Hydrologic Sciences Program (EAR-0405306 to D.S.M., EAR-0405381 to B.E.E., and EAR-0405318 to E.L.K.). In addition, M.M.L. was supported by the NSF IGERT program. The statements made in this manuscript reflect the views of the authors and do not necessary reflect the views of NSF. We are also grateful to personnel at Kemp Natural Resources Station, and to Dave Roberts for their assistance with field work. We wish to thank three anonymous reviewers whose comments helped improve earlier drafts of the manuscript.

References

Addington, R. N., R. J. Mitchell, R. Oren, and L. A. Donovan (2004), Stomatal sensitivity to vapor pressure deficit and its relationship to hydraulic conductance in pinus palustris, *Tree Physiol.*, *24*(5), 561–569.

Adelman, J. A., B. E. Ewers, and D. S. Mackay (2008), Using temporal patterns in vapor pressure deficit to explain spatial autocorrelation dynamics in tree transpiration, *Tree Physiol.*, *28*, 647–658.

Aranda, I., L. Gil, and J. A. Pardos (2005), Seasonal changes in apparent hydraulic conductance and their implications for water use of European beech (fagus sylvatica l.) and sessile oak [quercus petraea (matt.) liebl] in south Europe, *Plant Ecol.*, *179*(2), 155–167, doi:10.1007/s11258-004-7007-1.

Bakwin, P. S., P. P. Tans, D. F. Hurst, and C. L. Zhao (1998), Measurements of carbon dioxide on very tall towers: Results of the NOAA/CMDL program, *Tellus, Ser. B*, *50*(5), 401–415, doi:10.1034/j.1600-0889.1998.t01-4-00001.x.

Ball, J. T., I. E. Woodrow, and J. A. Berry (1987), A model predicting stomatal conductance and its contribution to the control of photosynthesis under different environmental conditions, in *Progress in Photosynthesis Research*, edited by J. Biggens, pp. 221–224, Martinus Nijhoff, Dordrecht, Netherlands.

Bella, I. E. (1971), A new competition model for individual trees, *For. Sci.*, *17*, 364–372.

Berger, U., and H. Hildenbrandt (2000), A new approach to spatially explicit modelling of forest dynamics: Spacing, ageing and neighbourhood competition of mangrove trees, *Ecol. Modell.*, *132*(5), 287–302, doi:10.1016/S0304-3800(00)00298-2.

Bonan, G. B. (1991), Atmosphere-biosphere exchange of carbon dioxide in boreal forests, *J. Geophys. Res.*, *96*(D4), 7301–7312, doi:10.1029/90JD02713.

Brodribb, T. J., and T. S. Feild (2000), Stem hydraulic supply is linked to leaf photosynthetic capacity: Evidence from new Caledonian and Tasmanian rainforests, *Plant Cell Environ.*, *23*(12), 1381–1388, doi:10.1046/j.1365-3040.2000.00647.x.

Burgess, S., and T. Dawson (2008), Using branch and basal trunk sap flow measurements to estimate whole-plant water capacitance: A caution, *Plant Soil*, *305*(1–2), 5–13, doi:10.1007/s11104-007-9378-2.

Burrows, S. N., S. T. Gower, M. K. Clayton, D. S. Mackay, D. E. Ahl, J. M. Norman, and G. Diak (2002), Application of geostatistics to characterize leaf area index (LAI) from flux tower to landscape scales using a cyclic sampling design, *Ecosystems*, *5*(7), 667–679.

Campbell, G. S., and J. M. Norman (1998), *An Introduction to Environmental Biophysics*, 2nd ed., pp. 247–263, Springer, New York.

Canham, C., P. Lepage, and K. Coates (2004), A neighborhood analysis of canopy tree competition: Effects of shading versus crowding, *Can. J. For. Res.*, *34*(4), 778–787, doi:10.1139/x03-232.

Cescatti, A. (1998), Effects of needle clumping in shoots and crowns on the radiative regime of a Norway spruce canopy, *Ann. Sci. For.*, *55*(1–2), 89–102, doi:10.1051/forest:19980106.

Chen, Q., D. D. Baldocchi, P. Gong, and T. Dawson (2008), Modeling radiation and photosynthesis of a heterogeneous savanna woodland landscape with a hierarchy of model complexities, *Agric. For. Meteorol.*, *148*(6–7), 1005–1020, doi:10.1016/j.agrformet.2008.01.020.

Clinger, W., and J. W. Vanness (1976), Unequally spaced time points in time-series, *Ann. Stat.*, *4*(4), 736–745, doi:10.1214/aos/1176343545.

Clinton, B. (2003), Light, temperature, and soil moisture responses to elevation, evergreen understory, and small canopy gaps in the southern Appalachians, *For. Ecol. Manage.*, *186*(1–3), 243–255, doi:10.1016/S0378-1127(03)00277-9.

Cochard, H., L. Coll, X. Le Roux, and T. Ameglio (2002), Unraveling the effects of plant hydraulics on stomatal closure during water stress in walnut, *Plant Physiol.*, *128*(1), 282–290, doi:10.1104/pp.010400.

Cook, B. D., et al. (2004), Carbon exchange and venting anomalies in an upland deciduous forest in northern Wisconsin, USA, *Agric. For. Meteorol.*, *126*(3–4), 271–295, doi:10.1016/j.agrformet.2004.06.008.

Courbaud, B. (2003), Simulating radiation distribution in a heterogeneous Norway spruce forest on a slope, *Agric. For. Meteorol.*, *116*(1–2), 1–18, doi:10.1016/S0168-1923(02)00254-X.

Davis, K. J., P. S. Bakwin, C. X. Yi, B. W. Berger, C. L. Zhao, R. M. Teclaw, and J. G. Isebrands (2003), The annual cycles of CO_2 and H_2O exchange over a northern mixed forest as observed from a very tall tower, *Global Change Biol.*, *9*(9), 1278–1293, doi:10.1046/j.1365-2486.2003.00672.x.

Denning, A. S., M. Nicholls, L. Prihodko, I. Baker, P. L. Vidale, K. Davis, and P. Bakwin (2003), Simulated variations in atmospheric CO_2 over a Wisconsin forest using a coupled ecosystem-atmosphere model, *Global Change Biol.*, *9*(9), 1241–1250, doi:10.1046/j.1365-2486.2003.00613.x.

de Pury, D. G. G., and G. D. Farquhar (1997), Simple scaling of photosynthesis from leaves to canopies without the errors of big-leaf models, *Plant Cell Environ.*, *20*(5), 537–557, doi:10.1111/j.1365-3040.1997.00094.x.

Ewers, B. E., and R. Oren (2000), Analyses of assumptions and errors in the calculation of stomatal conductance from sap flux measurements, *Tree Physiol.*, *20*(9), 579–589.

Ewers, B. E., R. Oren, N. Phillips, M. Stromgren, and S. Linder (2001), Mean canopy stomatal conductance responses to water and nutrient availabilities in picea abies and pinus taeda, *Tree Physiol.*, *21*(12–13), 841–850.

Ewers, B. E., D. S. Mackay, S. T. Gower, D. E. Ahl, S. N. Burrows, and S. S. Samanta (2002), Tree species effects on stand transpiration in northern Wisconsin, *Water Resour. Res.*, *38*(7), 1103, doi:10.1029/2001WR000830.

Ewers, B. E., S. T. Gower, B. Bond-Lamberty, and C. K. Wang (2005), Effects of stand age and tree species on canopy transpiration and average stomatal conductance of boreal forests, *Plant Cell Environ.*, *28*(5), 660–678, doi:10.1111/j.1365-3040.2005.01312.x.

Ewers, B. E., D. S. Mackay, and S. Samanta (2007a), Interannual consistency in canopy stomatal conductance control of leaf water potential across seven tree species, *Tree Physiol.*, *27*(1), 11–24.

Ewers, B. E., R. Oren, H. S. Kim, G. Bohrer, and C. T. Lai (2007b), Effects of hydraulic architecture and spatial variation in light on mean stomatal conductance of tree branches and crowns, *Plant Cell Environ.*, *30*(4), 483–496, doi:10.1111/j.1365-3040.2007.01636.x.

Ewers, B. E., D. Mackay, J. Tang, P. Bolstad, and S. Samanta (2008), Intercomparison of sugar maple (acer saccharum marsh.) stand transpiration responses to environmental conditions from the western Great Lakes region of the United States, *Agric. For. Meteorol.*, *148*(2), 231–246, doi:10.1016/j.agrformet.2007.08.003.

Famiglietti, J. S., and E. F. Wood (1994), Multiscale modeling of spatially variable water and energy-balance processes, *Water Resour. Res.*, *30*(11), 3061–3078, doi:10.1029/94WR01498.

Farquhar, G. D., S. Caemmerer, and J. A. Berry (1980), A biochemical model of photosynthetic CO_2 assimilation in leaves of C_3 species, *Planta*, *149*, 79–90.

Fassnacht, K. S., and S. T. Gower (1997), Interrelationships among the edaphic and stand characteristics, leaf area index, and aboveground net primary production of upland forest ecosystems in north central Wisconsin, *Can. J. For. Res.*, *27*(7), 1058–1067, doi:10.1139/cjfr-27-7-1058.

Foley, J. A., I. C. Prentice, N. Ramankutty, S. Levis, D. Pollard, S. Sitch, and A. Haxeltine (1996), An integrated biosphere model of land surface processes, terrestrial carbon balance, and vegetation dynamics, *Global Biogeochem. Cycles*, *10*(4), 603–628, doi:10.1029/96GB02692.

Franks, P. J. (2004), Stomatal control and hydraulic conductance, with special reference to tall trees, *Tree Physiol.*, *24*(8), 865–878.

Franks, P. J., P. L. Drake, and R. H. Froend (2007), Anisohydric but isohydrodynamic: Seasonally constant plant water potential gradient explained by a stomatal control mechanism incorporating variable plant hydraulic conductance, *Plant Cell Environ.*, *30*(1), 19–30, doi:10.1111/j.1365-3040.2006.01600.x.

Frelich, L. E., and C. G. Lorimer (1985), Current and predicted long-term effects of deer browsing in hemlock forests in Michigan, USA, *Biol. Conserv.*, *34*(2), 99–120, doi:10.1016/0006-3207(85)90103-X.

Gazal, R. M., R. L. Scott, D. C. Goodrich, and D. G. Williams (2006), Controls on transpiration in a semiarid riparian cottonwood forest, *Agric. For. Meteorol.*, *137*(1–2), 56–67, doi:10.1016/j.agrformet.2006.03.002.

Granier, A. (1987), Evaluation of transpiration in a douglas-fir stand by means of sap flow measurements, *Tree Physiol.*, *3*(4), 309–319.

Granier, A., P. Biron, and D. Lemoine (2000), Water balance, transpiration and canopy conductance in two beech stands, *Agric. For. Meteorol.*, *100*(4), 291–308, doi:10.1016/S0168-1923(99)00151-3.

Jarvis, P. G. (1976), Interpretation of variations in leaf water potential and stomatal conductance found in canopies in field, *Philos. Trans. R. Soc. London, Ser. B*, *273*(927), 593–610, doi:10.1098/rstb.1976.0035.

Jones, T., and S. Thomas (2007), Leaf-level acclimation to gap creation in mature acer saccharum trees, *Tree Physiol.*, *27*(2), 281.

Katul, G., D. Ellsworth, and C. Lai (2000), Modelling assimilation and intercellular CO_2 from measured conductance: A synthesis of approaches, *Plant Cell Environ.*, *23*(12), 1313–1328, doi:10.1046/j.1365-3040.2000.00641.x.

Katul, G., R. Leuning, and R. Oren (2003), Relationship between plant hydraulic and biochemical properties derived from a steady-state coupled water and carbon transport model, *Plant Cell Environ.*, *26*(3), 339–350, doi:10.1046/j.1365-3040.2003.00965.x.

Katul, G., S. Palmroth, and R. Oren (2009), Leaf stomatal responses to vapor pressure deficit under current and CO_2-enriched atmosphere explained by the economics of gas exchange, *Plant Cell Environ.*, *32*, 968–979, doi:10.1111/j.1365-3040.2009.01977.x.

Kuchment, L., and V. Demidov (2006), Modeling of influence of hydrological processes on the carbon cycle of a forest ecosystem, *Environ. Model. Softw.*, *21*(1), 111–114, doi:10.1016/j.envsoft.2005.01.002.

Kuchment, L., V. Demidov, and Z. Startseva (2006), Coupled modeling of the hydrological and carbon cycles in the soil-vegetation-atmosphere system, *J. Hydrol.*, *323*(1–4), 4–21, doi:10.1016/j.jhydrol.2005.08.011.

Kumagai, T. (2008), Transpiration and canopy conductance at two slope positions in a Japanese cedar forest watershed, *Agric. For. Meteorol.*, *148*(10), 1444–1455, doi:10.1016/j.agrformet.2008.04.010.

Lagergren, F., and A. Lindroth (2002), Transpiration response to soil moisture in pine and spruce trees in Sweden, *Agric. For. Meteorol.*, *112*(2), 67–85, doi:10.1016/S0168-1923(02)00060-6.

Lagergren, F., and A. Lindroth (2004), Variation in sapflow and stem growth in relation to tree size, competition and thinning in a mixed forest of pine and spruce in Sweden, *For. Ecol. Manage.*, *188*(1–3), 51–63, doi:10.1016/j.foreco.2003.07.018.

Landsberg, J. J., and R. H. Waring (1997), A generalised model of forest productivity using simplified concepts of radiation-use efficiency, carbon balance and partitioning, *For. Ecol. Manage.*, *95*(3), 209–228, doi:10.1016/S0378-1127(97)00026-1.

Lappi, J., and P. Stenberg (1998), Joint effect of angular distribution of radiation and spatial pattern of trees on radiation interception, *Ecol. Modell.*, *112*(1), 45–51, doi:10.1016/S0304-3800(98)00112-4.

Larocque, G. R. (2002), Coupling a detailed photosynthetic model with foliage distribution and light attenuation functions to compute daily gross photosynthesis in sugar maple (acer saccharum marsh.) stands, *Ecol. Modell.*, *148*(3), 213–232, doi:10.1016/S0304-3800(01)00442-2.

Lei, T. T., and M. J. Lechowicz (1997), The photosynthetic response of eight species of acer to simulated light regimes from the centre and edges of gaps, *Funct. Ecol.*, *11*(1), 16–23, doi:10.1046/j.1365-2435.1997.00048.x.

Long, S. P., and C. J. Bernacchi (2003), Gas exchange measurements, what can they tell us about the underlying limitations to photosynthesis? Procedures and sources of error, *J. Exp. Bot.*, *54*(392), 2393–2401, doi:10.1093/jxb/erg262.

Loranty, M. M., D. S. Mackay, B. E. Ewers, J. D. Adelman, and E. L. Kruger (2008), Environmental drivers of spatial variation in whole-tree transpiration in an aspen-dominated upland-to-wetland forest gradient, *Water Resour. Res.*, *44*, W02441, doi:10.1029/2007WR006272.

Lorimer, C. G. (1983), Tests of age-independent competition indices for individual trees in natural hardwood stands, *For. Ecol. Manage.*, *6*(4), 343–360, doi:10.1016/0378-1127(83)90042-7

Mackay, D. S., D. E. Ahl, B. E. Ewers, S. T. Gower, S. N. Burrows, S. Samanta, and K. J. Davis (2002), Effects of aggregated classifications of forest composition on estimates of evapotranspiration in a northern Wisconsin forest, *Global Change Biol.*, *8*(12), 1253–1265, doi:10.1046/j.1365-2486.2002.00554.x.

Mackay, D. S., D. E. Ahl, B. E. Ewers, S. Samanta, S. T. Gower, and S. N. Burrows (2003), Physiological tradeoffs in the parameterization of a model of canopy transpiration, *Adv. Water Resour.*, *26*(2), 179–194, doi:10.1016/S0309-1708(02)00090-8.

Mackay, D. S., B. E. Ewers, B. D. Cook, and K. J. Davis (2007), Environmental drivers of evapotranspiration in a shrub wetland and an upland forest in northern Wisconsin, *Water Resour. Res.*, *43*, W03442, doi:10.1029/2006WR005149.

Maherali, H., M. Sherrard, M. Clifford, and R. Latta (2008), Leaf hydraulic conductivity and photosynthesis are genetically correlated in an annual grass, *New Phytol.*, *180*(1), 240–247, doi:10.1111/j.1469-8137.2008.02548.x.

McDowell, N., et al. (2002), The relationship between tree height and leaf area: Sapwood area ratio, *Oecologia*, *132*(1), 12–20, doi:10.1007/s00442-002-0904-x.

Monteith, J. L. (1965), Evaporation and the environment, in *Proceedings of the 19th Symposium of the Society for Experimental Biology*, Cambridge Univ. Press, New York.

Monteith, J. L., and M. H. Unsworth (1990), *Principles of Environmental Physics*, 2nd ed., Chapman and Hall, New York.

Moore, G. W., B. J. Bond, J. A. Jones, N. Phillips, and F. C. Meinzer (2004), Structural and compositional controls on transpiration in 40- and 450-year-old riparian forests in western Oregon, USA, *Tree Physiol.*, *24*(5), 481–491.

Mott, K. A., and D. F. Parkhurst (1991), Stomatal response to humidity in air and helox, *Plant Cell Environ.*, *14*, 509–515, doi:10.1111/j.1365-3040.1991.tb01521.x.

Naidu, S. L., and E. H. Delucia (1997), Acclimation of shade-developed leaves on saplings exposed to late-season canopy gaps, *Tree Physiol.*, *17*(6), 367–376.

Niinemets, U., O. Kull, and J. D. Tenhunen (2004), Within-canopy variation in the rate of development of photosynthetic capacity is proportional to integrated quantum flux density in temperate deciduous trees, *Plant Cell Environ.*, *27*(3), 293–313, doi:10.1111/j.1365-3040.2003.01143.x.

Novick, K., R. Oren, P. Stoy, J.-Y. Juang, M. Siqueira, and G. Katul (2009), The relationship between reference canopy conductance and simplified hydraulic architecture, *Adv. Water Resour.*, *32*(6), 809–819, doi:10.1016/j.advwatres.2009.02.004.

Oishi, A., R. Oren, and P. Stoy (2008), Estimating components of forest evapotranspiration: A footprint approach for scaling sap flux measurements, *Agric. For. Meteorol.*, *148*(11), 1719–1732, doi:10.1016/j.agrformet.2008.06.013.

Oren, R., and D. E. Pataki (2001), Transpiration in response to variation in microclimate and soil moisture in southeastern deciduous forests, *Oecologia*, *127*(4), 549–559, doi:10.1007/s004420000622.

Oren, R., N. Phillips, G. Katul, B. E. Ewers, and D. E. Pataki (1998), Scaling xylem sap flux and soil water balance and calculating variance: A method for partitioning water flux in forests, *Ann. Sci. For.*, *55*(1–2), 191–216, doi:10.1051/forest:19980112.

Oren, R., N. Phillips, B. E. Ewers, D. E. Pataki, and J. P. Megonigal (1999a), Sap-flux-scaled transpiration responses to light, vapor pressure deficit, and leaf area reduction in a flooded taxodium distichum forest, *Tree Physiol.*, *19*(6), 337–347.

Oren, R., J. S. Sperry, G. G. Katul, D. E. Pataki, B. E. Ewers, N. Phillips, and K. V. R. Schafer (1999b), Survey and synthesis of intra- and interspecific variation in stomatal sensitivity to vapour pressure deficit, *Plant Cell Environ.*, *22*(12), 1515–1526, doi:10.1046/j.1365-3040.1999.00513.x.

Pataki, D. E., R. Oren, and W. K. Smith (2000), Sap flux of co-occurring species in a western subalpine forest during seasonal soil drought, *Ecology*, *81*(9), 2557–2566, doi:10.1890/0012-9658(2000)081[2557:SFOCOS]2.0.CO;2.

Perala, D. A., and D. H. Alban (1994), Allometric biomass estimators for aspen-dominated ecosystems in the Upper Great Lakes, *U.S. For. Serv. Res. Pap.*, *NC-134*, 38.

Phillips, N., and R. Oren (1998), A comparison of daily representations of canopy conductance based on two conditional time-averaging methods and the dependence of daily conductance on environmental factors, *Ann. Sci. For.*, *55*(1–2), 235, doi:10.1051/forest:19980113.

Phillips, N., F. Scholz, S. Bucci, G. Goldstein, and F. Meinzer (2009), Using branch and basal trunk sap flow measurements to estimate whole-plant water capacitance: Comment on Burgess and Dawson (2008), *Plant Soil*, *315*(1–2), 315–324, doi:10.1007/s11104-008-9741-y.

Porté, A., F. Huard, and P. Dreyfus (2004), Microclimate beneath pine plantation, semi-mature pine plantation and mixed broadleaved-pine forest, *Agric. For. Meteorol.*, *126*(1–2), 175–182, doi:10.1016/j.agrformet.2004.06.001.

Raulier, F., P. Y. Bernier, C. H. Ung, and R. Boutin (2002), Structural differences and functional similarities between two sugar maple (acer saccharum) stands, *Tree Physiol.*, *22*(15–16), 1147–1156.

Running, S. W., and J. C. Coughlan (1988), A general-model of forest ecosystem processes for regional applications. 1. Hydrologic balance, canopy gas-exchange and primary production processes, *Ecol. Modell.*, *42*(2), 125–154, doi:10.1016/0304-3800(88)90112-3.

Samanta, S., and D. S. Mackay (2003), Flexible automated parameterization of hydrologic models using fuzzy logic, *Water Resour. Res.*, *39*(1), 1009, doi:10.1029/2002WR001349.

Samanta, S., D. S. Mackay, M. K. Clayton, E. L. Kruger, and B. E. Ewers (2007), Bayesian analysis for uncertainty estimation of a canopy transpiration model, *Water Resour. Res.*, *43*, W04424, doi:10.1029/2006WR005028.

Samanta, S., M. K. Clayton, D. S. Mackay, E. L. Kruger, and B. E. Ewers (2008), Quantitative comparison of canopy conductance models using a Bayesian approach, *Water Resour. Res.*, *44*, W09431, doi:10.1029/2007WR006761.

Schafer, K. V. R., R. Oren, and J. D. Tenhunen (2000), The effect of tree height on crown level stomatal conductance, *Plant Cell Environ.*, *23*(4), 365–375, doi:10.1046/j.1365-3040.2000.00553.x.

Sperry, J. S., F. R. Adler, G. S. Campbell, and J. P. Comstock (1998), Limitation of plant water use by rhizosphere and xylem conductance: Results from a model, *Plant Cell Environ.*, *21*(4), 347–359, doi:10.1046/j.1365-3040.1998.00287.x.

Spitters, C. J. T., H. Toussaint, and J. Goudriaan (1986), Separating the diffuse and direct component of global radiation and its implications for modeling canopy photosynthesis. Part I. Components of incoming radiation, *Agric. For. Meteorol.*, *38*, 217–229, doi:10.1016/0168-1923(86)90060-2.

Stoy, P., G. Katul, M. Siqueira, J. Juang, K. Novick, H. McCarthy, A. C. Oishi, J. Uebelherr, H. Kim, and R. Oren (2006), Separating the effects of climate and vegetation on evapotranspiration along a successional chronosequence in the southeastern US, *Global Change Biol.*, *12*(11), 2115–2135, doi:10.1111/j.1365-2486.2006.01244.x.

Tardieu, F., and T. Simonneau (1998), Variability among species of stomatal control under fluctuating soil water status and evaporative demand: Modelling isohydric and anisohydric behaviours, *J. Exp. Bot.*, *49*, 419–432, doi:10.1093/jexbot/49.suppl_1.419.

Traver, E. T., B. E. Ewers, D. S. Mackay, and M. M. Loranty (2010), Tree transpiration varies spatially in response to atmospheric but edaphic conditions, *Funct. Ecol.*, *24*(2), 273–282, doi:10.1111/j.1365-2435.2009.01657.x.

Tromp-van Meerveld, H. J., and J. J. McDonnell (2006), On the interrelations between topography, soil depth, soil moisture, transpiration rates and species distribution at the hillslope scale, *Adv. Water Resour.*, *29*(2), 293–310, doi:10.1016/j.advwatres.2005.02.016.

Tyree, M. T., and J. S. Sperry (1989), Vulnerability of xylem to cavitation and embolism, *Annu. Rev. Plant Physiol. Plant Mol. Biol.*, *40*, 19–38, doi:10.1146/annurev.pp.40.060189.000315.

Walcroft, A. S., D. Whitehead, F. M. Kelliher, A. Arneth, and W. B. Silvester (2002), The effects of long-term, partial shading on growth and photosynthesis in *Pinus radiata* D. Don trees, For. *Ecol. Manage.*, *163*(1–3), 151–163, doi:10.1016/S0378-1127(01)00540-0.

Wang, Y., D. D. Baldocchi, R. Leuning, E. Falge, and T. Vesala (2007), Estimating parameters in a land-surface model by applying nonlinear inversion to eddy covariance flux measurements from eight fluxnet sites, *Global Change Biol.*, *13*(3), 652–670, doi:10.1111/j.1365-2486.2006.01225.x.

Whitehead, D., and P. G. Jarvis (1981), Coniferous forests and plantations, in *Water Deficits and Plant Growth*, edited by T. T. Kowlowski, pp. 49–152, Academic, San Diego, Calif.

Whitehead, D., W. R. N. Edwards, and P. G. Jarvis (1984), Conducting sapwood area, foliage area, and permeability in mature trees of picea-sitchensis and pinus-contorta, *Can. J. For. Res.*, *14*(6), 940–947, doi:10.1139/x84-166.

Williams, D. G., et al. (2004), Evapotranspiration components determined by stable isotope, sap flow and eddy covariance techniques, *Agric. For. Meteorol.*, *125*(3–4), 241–258, doi:10.1016/j.agrformet.2004.04.008.

Willmott, C. J. (1982), Some comments on the evaluation of model performance, *Bull. Am. Meteorol. Soc.*, *63*(11), 1309–1313, doi:10.1175/1520-0477(1982)063<1309:SCOTEO>2.0.CO;2.

Woodruff, D., K. McCulloh, J. Warren, F. Meinzer, and B. Lachenbruch (2007), Impacts of tree height on leaf hydraulic architecture and stomatal control in douglas-fir, *Plant Cell Environ.*, *30*(5), 559–569, doi:10.1111/j.1365-3040.2007.01652.x.

Wullschleger, S. D., P. J. Hanson, and D. E. Todd (2001), Transpiration from a multi-species deciduous forest as estimated by xylem sap flow

techniques, *For. Ecol. Manage.*, *143*(1–3), 205–213, doi:10.1016/S0378-1127(00)00518-1.

Wullschleger, S. D., C. A. Gunderson, P. J. Hanson, K. B. Wilson, and R. J. Norby (2002), Sensitivity of stomatal and canopy conductance to elevated CO_2 concentration: Interacting variables and perspectives of scale, *New Phytol.*, *153*(3), 485–496, doi:10.1046/j.0028-646X.2001.00333.x.

B. E. Ewers, Department of Botany, University of Wyoming, 1000 E. University Ave., Laramie, WY 82071, USA.

E. L. Kruger, Department of Forest Ecology and Management, University of Wisconsin-Madison, 1630 Linden Dr., Madison, WI 53706, USA.

M. M. Loranty, Woods Hole Research Center, 149 Woods Hole Rd., Falmouth, MA 02540, USA. (mloranty@whrc.org)

D. S. Mackay, Department of Geography, State University of New York at Buffalo, 105 Wilkeson Quadrangle, Buffalo, NY 14261, USA.

E. Traver, Department of Biological Sciences, Dartmouth College, Hanover, NH 03755, USA.